We are IntechOpen,
the world's leading publisher of
Open Access books
Built by scientists, for scientists

6,900
Open access books available

186,000
International authors and editors

200M
Downloads

Our authors are among the

154
Countries delivered to

TOP 1%
most cited scientists

12.2%
Contributors from top 500 universities

CLARIVATE ANALYTICS
BOOK CITATION INDEX
INDEXED

WEB OF SCIENCE™

Selection of our books indexed in the Book Citation Index
in Web of Science™ Core Collection (BKCI)

Interested in publishing with us?
Contact book.department@intechopen.com

Numbers displayed above are based on latest data collected.
For more information visit www.intechopen.com

Calorimetric: A Tecnique Useful in Characterization of Porous Solid

Juan Carlos Moreno[1] and Liliana Giraldo[2]
[1]Universidad de los Andes, Bogotá,
[2]Universidad Nacional de Colombia, Bogotá
Colombia

1. Introduction

The adsorption of gases in porous solids such as zeolites and activated carbons, has been widely applied in cases of separation, purification and bottling of gases (Ruthven et al. 1994; Yang, 1997; Bastos-Neto et al. 2005a; Figueroa et al., 2008; Belmabkhout and Sayari, 2009). This potential is reflected not only in increasing the number of technical and scientific articles and patents, but also in the world market growth in plants for air separation and purification processes of hydrogen and natural gas and many others (Zimmermann and Keller, 2003). Due to the various applications of porous adsorbents, many research groups in various parts of the world have sought to develop and improve these materials to improve performance in these specific applications (Bastos-Neto et al. 2005b; Arou et al., 2008; Prauchner and Rodriguez-Reinoso, 2008; Rivers and Smith, 2009). In the procedures for obtaining porous solids, it is necessary to control the various process variables such as preparation, carbonization temperature and time, type and concentration of activating agents, among others, since these activation parameters determine the chemical and physical properties of adsorbents. The textural characteristics are the most important properties of the adsorbents, since it indicates the implementation and performance of the solid obtained (Giraldo and Moreno, 2005). In addition, chemical properties also determine the adsorption properties of adsorbent and solid-fluid interactions. Nature of surface groups, hydrophobic or hydrophilic character and acidic or basic behavior are some of the relevant chemical properties of the adsorbents in adsorption processes. Since the physical and chemical properties of an adsorbent determine the application and performance of the same, it is necessary to determine precisely the parameters that characterize these materials such as surface area, microporosity, pore size distribution, heats of adsorption, among others. Several experimental techniques are used to characterize porous materials, for example, mercury porosimetry, adsorption of liquid nitrogen, x-ray diffraction, etc.. The technique most commonly used to characterize the texture of carbon adsorbents (ie surface area, properties of molecular sieve, size distribution of pores, etc.). Is the physical adsorption of gases and vapors. However, immersion calorimetry, with molecular probes of various molecular dimensions, and gas adsorption microcalorimetry techniques are also applied to characterize this type of solid (Denoyel et al., 1993, González et al. 1995; Rouquerol et al. 1999, Navarrete et al., 2004; Garcia-Cuello et al., 2009). The aim of this

study is to review the calorimetric methods as a technique for characterization of adsorbent materials. The focus of this study is to review available scientific articles in the literature showing the use of calorimetry to physical characterization of adsorbent materials. The aim is also to describe some types of calorimeters commonly used in adsorption processes.

2. Adsorption calorimetry

The determination of heat of adsorption is essential in the description of gas solid interactions. This is particularly useful when measuring the heat of adsorption are combined with simultaneous measurements of adsorption isotherm (Llewellyn and Maurin, 2005; Garcia-Cuello et al., 2008; Garcia-Cuello et al., 2009). There are many factors to determine the heat of adsorption, namely: to characterize the surface energy of the material (Rouquerol et al., 1999); provide basic data for developing new theories for equilibrium and kinetic adsorption (Zimmermann and Keller, 2003); design and improve plants separation processes such as adsorption and desorption, PSA, VSA, TSA and their combinations (Ruthven et al. 1984; Yang, 1997). Calorimetry was never widely used for characterization of carbons. In fact, its use has been limited to a few researchers who have used calorimetric techniques to specific problems (Menéndez, 1998). However, it has been shown that the adsorption calorimetry in combination with other physical techniques or physical-chemical properties can be used to describe the properties of the surface of a solid (Llewellyn and Maurin, 2005; Giraldo and Moreno, 2005; Garcia-Cuello et al., 2008; Garcia-Cuello et al., 2009). Menéndez (1998) presents a brief review of calorimetric methods applied to physical and chemical surface characterization of carbonaceous adsorbents. Their results indicate great potential of using calorimetry to study the physical structure (ie textural) of carbons, especially when used in conjunction with more traditional techniques based on physical adsorption of gases and vapors. Three types of calorimetric methods have been used to characterize the porous solids, namely, immersion, flow-adsorption calorimetry and gas adsorption. Among the three methods, immersion calorimetry and itrogen adsorption are the most used for the characterization of adsorbents. The next section presents the classifications of the calorimetric curves depending on the classification of adsorption isotherms according to IUPAC. In the following sections will show the advantages of using calorimetric techniques as a tool for characterization of adsorbents through their applications.

2.1 Theoretical microcalorimetric curves (Llewellyn and Maurin, 2005)

The differential enthalpy curve obtained from microcalorimetric experiments is a result of various effects that include both adsorbent-adsorbate interactions and adsorbate-adsorbate. Mechanisms of pore filling and phase transition can be demonstrated as well as structural changes of the adsorbent. In general, the calorimetric curve shows three distinct behaviors, as shown in Figure 1. In each system, an increased amount of gas adsorbed by the sample leads to an increase of interactions between adsorbed molecules. Regarding contributions adsorbate-adsorbent, the interaction of the adsorbed molecule with an energetically homogeneous surface leads to a constant signal.

Finally, in most cases, the adsorbent is energetically heterogeneous due to their pore size distribution (amorphous adsorbents) or a variable surface chemistry (defects, cations, etc.).. Initially, one would expect relatively strong interactions between the adsorbed molecules and surface. The intensity of these interactions decreases as the specific sites are occupied.

Therefore, to energetically heterogeneous adsorbents, a gradual decrease in the calorimetric signal is observed. However, each curve of enthalpy differential current varies because the results of the different contributions are summed.
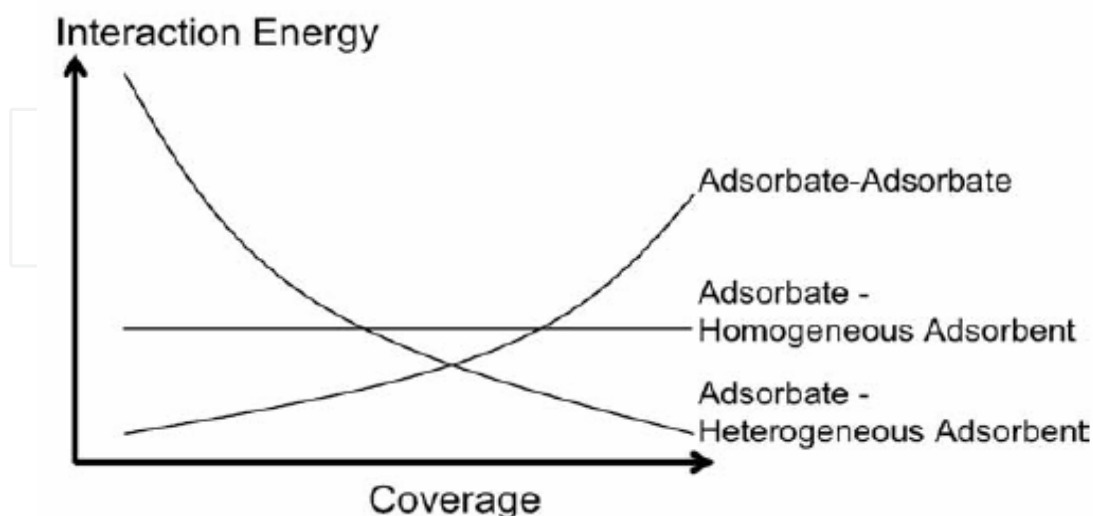

Fig. 1. Hypothetical calorimetric curves illustring the various interactions involved during the adsorption of simple gases at low temperatures . (Llewellyn and Maurin, 2005.)

2.2 Thermodynamic basis of calorimetry

The determination of the heat quantity that is involved in a process, be it physical, chemical, or biological, provides information about the evolution, duration, and intensity of the same, and the experimentation being conducted to determine the magnitude of the heat that is produced or absorbed can be simple or complex according to the required measurement accuracy, the sensitivity of the instruments used, and the amount of energy that is transferred, to name some of the features involved in the determination.

In the development of chemistry, and particularly in the field of thermodynamics, calorimetry has been a factor of undeniable importance. Some authors point to the calorimeter as an instrument that opens up the second part of the pre-classical thermodynamics, which is called calorimetry (Swietoslawski, 1946).

Construction of the first calorimeter by Cavendish (Armstrong, 1964) in 1720, for the determination of the heat of vaporization of water and specific heats of various substances, was the start of the creation of a great variety of designs by leading researchers of that time, among whom names of such importance as Lavoisier, LaPlace, Black and Irvine, Bunsen, Dulong and Petit, and Nernst Euken can be highlighted (Wilhoit, 1967; Rouquerol, 1985).

Due to the large number of systems, phenomena, and conditions of interest, there is no single model of calorimeter, so their diversity is very wide. That is why since the very emergence of calorimeters a variety of equipment has been generated, among which we can examine adiabatic calorimeters, isothermal calorimeters, and isoperibolic calorimeters. In parallel with the development of calorimeters, it was necessary to improve data collection systems, leading to the use of peripheral systems with high sensitivity and precision.

The purposes and applications of calorimeters have greatly expanded the field of study and concepts of calorimetry and therefore of thermodynamics: the heat of solution, combustion, mixing, and vaporization are just some of the determinations that are made using this technique. Because information can be obtained from the measurement of heat, the number

of instrument designs for its determination has increased, taking into account that the energetic effect associated with different interactions may be of short duration or, later in development, hours or even weeks (Swietoslawski, 1946; Hemminger and Hohne, 1984).

The calorimetric determination must then take into account the accuracy required, the temperature, the amount of sample available, the magnitude of the heat involved, the duration of the experiment, and the cost of the instrument.

2.3 General classes and types of signals of calorimeters

The heat transfer can be determined in different conditions, and therefore different kinds of instruments are used as calorimeters, which can be classified into three general groups as described below (Wadso and Goldberg, 2001; Giraldo et al., 1996).

2.3.1 Isoperibolic calorimeter

An isoperibolic calorimeter maintains a constant temperature of the surroundings through the use of a thermostat, while the temperature measurement system may vary over time. There is a thermal resistance R_T, with a magnitude defined between the surroundings and the cell which is being measured, so that the heat exchange depends on the temperature difference between the temperature of the surroundings T_A and the temperature of the cell and measuring system T_C; as T_A is constant then the flow of heat is a function of T_C. If the heat generation within the cell is completed, the temperature T_C approaches the temperature of the surroundings T_A.
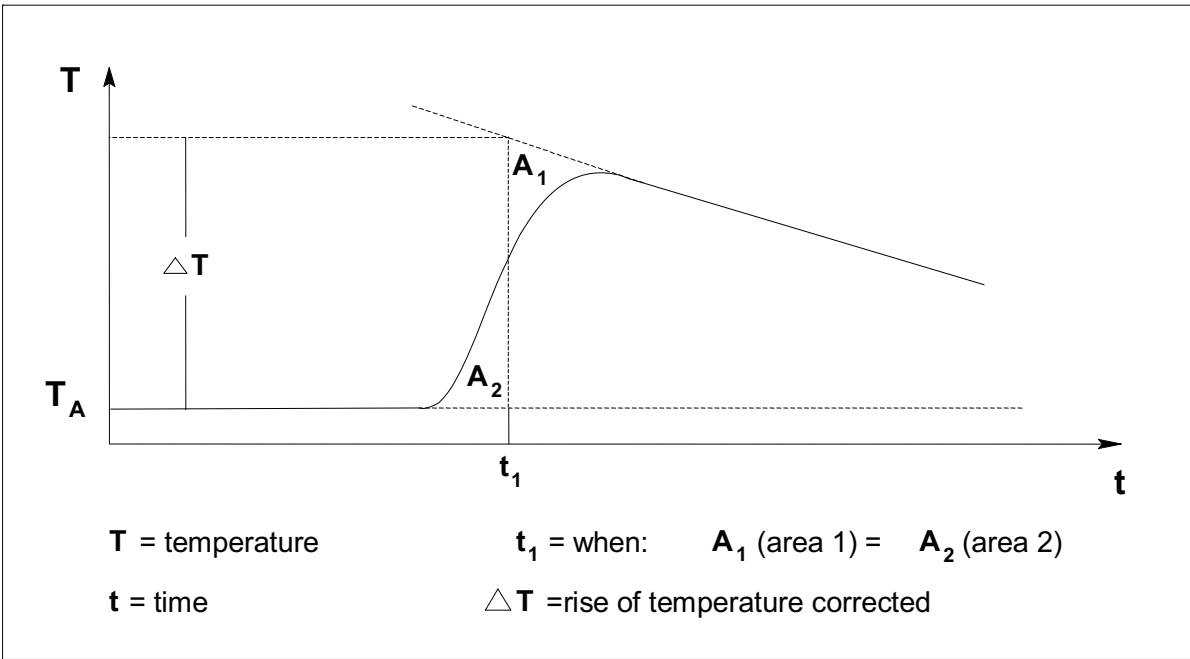

Fig. 2. Typical thermogram determined by an isoperibolic calorimeter. Adapted from Hohne et al. (1996)

Figure 2 illustrates a typical curve of temperature versus time obtained by an isoperibolic calorimeter in the observation of an exothermic event. At the beginning of the experiment the temperature stays close to the temperature of the surroundings T_A; when there is a certain amount of heat in the cell, the temperature increases initially, and then reaches a maximum value to finally begin to decline because T_A is less than T_C, and the magnitude of

the decrease depends on the isolation of the cell, that is, the thermal resistance R_T, which defines the constant heat leak, K_{ft}, a parameter of the device used, which is also a function of the temperature gradient. The amount of heat for the process under consideration is equal to $Q = Cp\Delta T_{corrected}$ where Cp is the heat capacity of the system understudy plus the heat capacity of the cell; ΔTcorrected is the difference in temperature above which gives a correction graphic of small but existing heat leaks, as shown in Figure 1. For accurate measurements it is not absolutely necessary to keep the heat losses as small as possible; however these are reproducible in terms of the temperature difference between the cell and the surrounding area and can be determined by electric calibration (Giraldo et al., 1994).

Taking into account the above considerations in general, isoperibolic calorimeters seek to reduce the heat exchange between the cell where the process is carried out and the surroundings, which is achieved by minimizing the temperature difference between them, decreasing the coefficient of heat transfer, and reducing the duration of heat exchange (Moreno and Giraldo, 2005).

2.3.2 Adiabatic calorimeters

Adiabatic calorimeters further restrict the heat transfer compared with isoperibolic calorimeters; ideally adiabatic calorimeters do not allow heat exchange between the cell and its surroundings. We can consider three ways to achieve this goal:
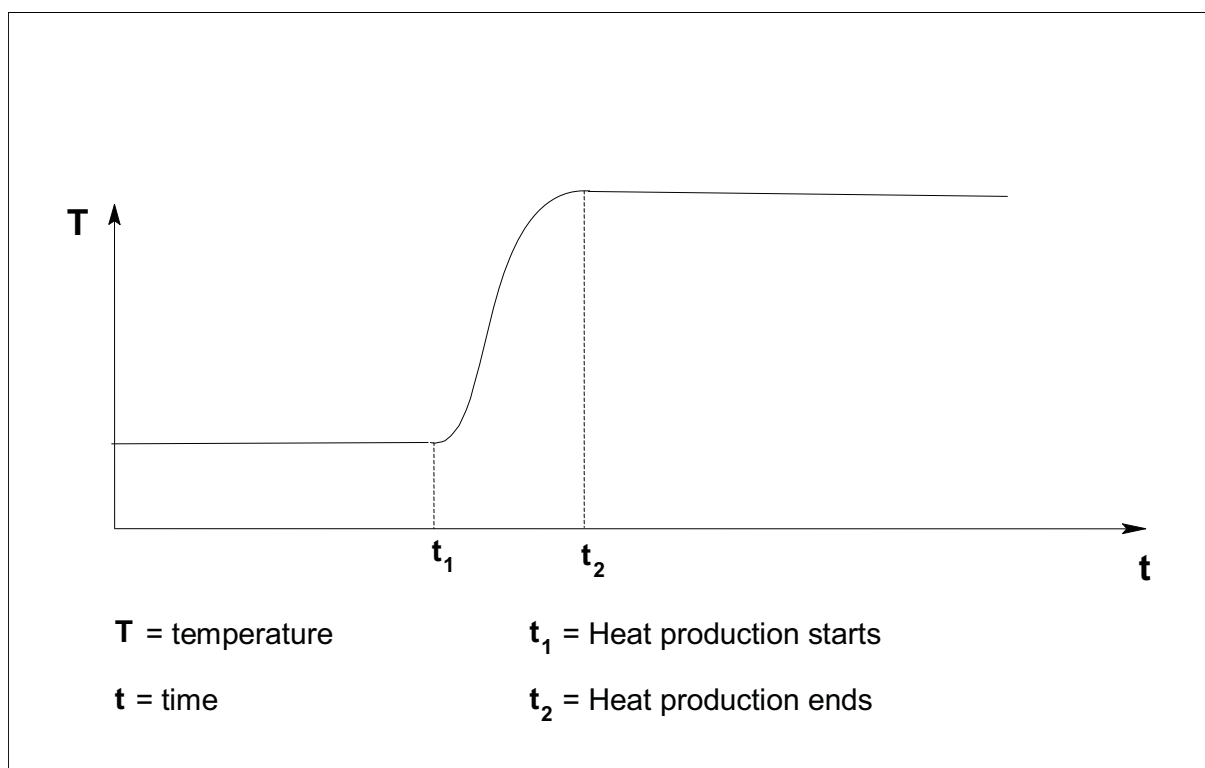

Fig. 3. Typical thermogram of an adiabatic calorimeter. Adapted from Hohne et al. (1996)

1. by carrying out the heat generation so fast that no appreciable amount of heat can enter or leave the cell during the period in which it is carried out;
2. by separating the cell to give a near to infinitely large thermal resistance R_T, so that the system is as isolated as possible;

3. by means of external controls that make the temperature of the surroundings always as close as possible to that of the cell.

During the calorimetric process any heat generated or consumed in the cell leads to a change in temperature. Figure 3 shows the graph of temperature versus time, T vs t. t_1 is generated in a heat effect until t_2. The Δheat can be calculated from measurements of the temperature difference ΔT:

$$Q = Cp\Delta T \tag{1}$$

The heat capacity is easily determined by calibration with the use of electricity. Ideally the slope of the curve of temperature versus time is proportional to heat flow:

$$\frac{dQ}{dt}(t) \approx C\frac{dT}{dt}(t) \tag{2}$$

where the heat flow dQ/dt (t) is obtained directly from curves like that shown in Figure 2.

2.3.3 Isothermal calorimeters

Another way of measuring the energy involved in a process, using a method opposed to the previous two (total isolation in the adiabatic case or allowing a small thermal leak in the isoperibolic case), provides a large exchange of the heat that is produced in the cell. This method is isothermal in nature, and the cell and its surroundings have the same constant temperature ($T_A = T_C$ = constant).

T = temperature t_1 = Heat production

t = time T_A = Surroundings temperature
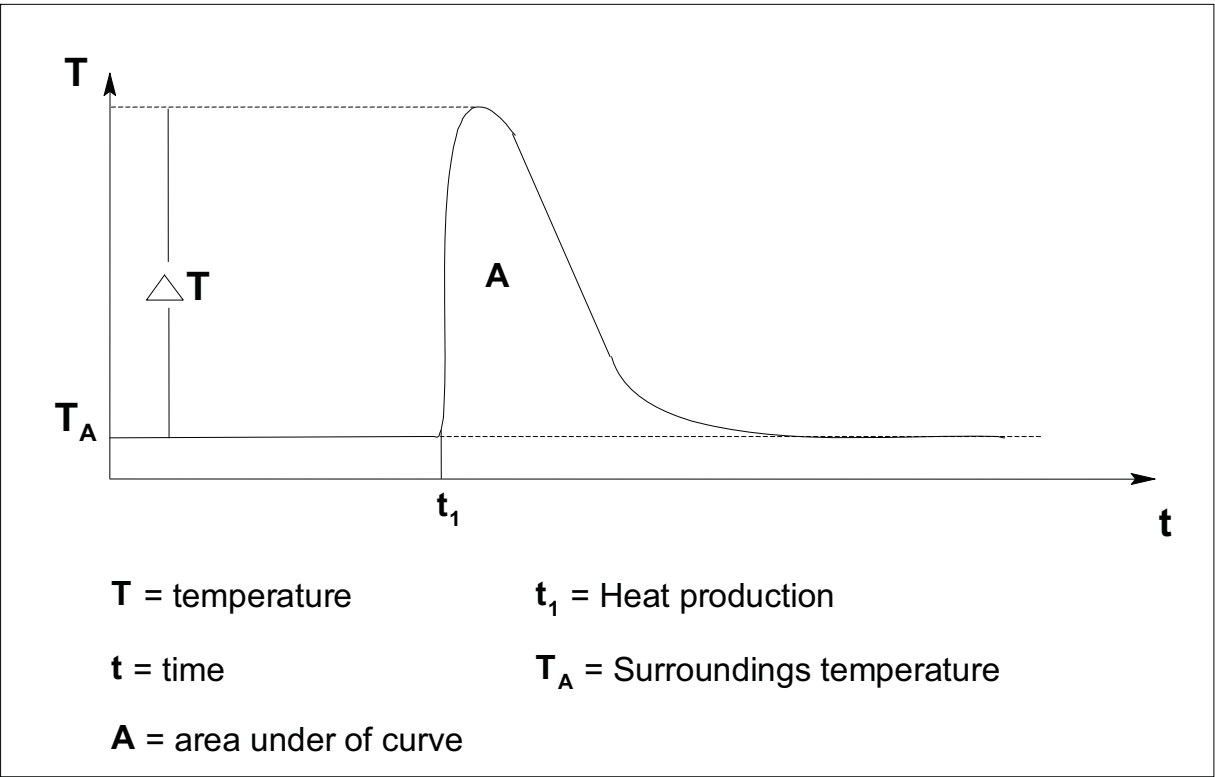
A = area under of curve

Fig. 4. Typical thermogram of an isothermal calorimeter. Adapted from Hohne et al. (1996)

The isothermal calorimeter has a very small thermal resistance R_T and also the heat capacity of the surrounding area is infinitely large. Taking into account these requirements, under strict conditions isothermal T_A and T_C may remain constant over time and space, but then no heat flow occurs. In real cases, we present a heat flow between the cell, and the surrounding flow is detected by thermal sensors placed between them. The flow is usually due to the small temperature difference between T_A and T_C during the process observed, and the magnitude of this temperature difference depends on the amount of heat released per unit time, the thermal conductivity and geometry of the cell, and the type of insulation of the thermal sensors. Despite these limitations, an isothermal calorimeter design is commonly used where temperatures T_A and T_C may be different from each other but each taken separately is constant throughout the duration of the process that generates the heat flow (Zielenkiewicz, 2000). Figure 4 shows a thermogram (T vs t) obtained with an isothermal calorimeter, where the heat conduction is observed around the drop in temperature after the cell is supplied with a pulse of heat.

2.3.4 Heat conduction calorimetry

Heat conduction calorimetry studies can be undertaken to provide kinetic and analytical thermodynamic data. The potential of the technique is such that Buckton (1995) states "The isothermal microcalorimetry has the ability to record all physical and chemical processes. The range of application of this technique is limited only by the imagination of the researcher and the ability to control the experiment." Some other interesting examples of applications of the technique are presented below.

Heat conduction calorimetry is classified as an isothermal technique (Wadso, 1986) because the variable that is constant in the experiment is the temperature of different parts of the computer. However, there is a local temperature difference which occurs whenever there is heat exchange between the cell and the surroundings (Wadso, 2001), as the heart of the device is composed of the cell, sensors, and a solid body, and this is expected to be the primary mechanism driving the exchange of heat.

In isothermal calorimetry, the surroundings and the cell have the same constant temperature:

$$T_{surrounding} = T_{cell} = constant \tag{3}$$

It can be seen that the calorimeter has a heat resistance, R_T, which is very small and also that the heat capacity of the surrounding area is infinitely large. Taking into account these requirements, under strictly isothermal conditions $T_{surrounding}$ and T_{cell} can remain constant over time and space, but then no heat flow occurs. In real cases, we present a heat flow between the cell and the surrounding flow is detected by thermal sensors placed between them. The flow is usually due to the small temperature difference between T_{cell} and $T_{surrounding}$, and during the process observed the magnitude of this temperature difference depends on the amount of heat released per unit time, the thermal conductivity and geometry of the cell, and the type of insulation of the thermal sensors (Hemminger and Hohne, 1984). Despite these limitations, isothermal calorimeters commonly have a design where the temperatures T_{cell} and $T_{surrounding}$ may differ from each other, but each taken separately is constant throughout the duration of the process that generates the heat flow.

Figure 5 shows a diagram of the arrangement of the measuring cell and the surroundings in a heat conduction calorimeter. The cell is connected with them through a thermal resistance R_T, which is an interesting parameter because it relates the flow of heat dQ/dt to the difference in temperature.
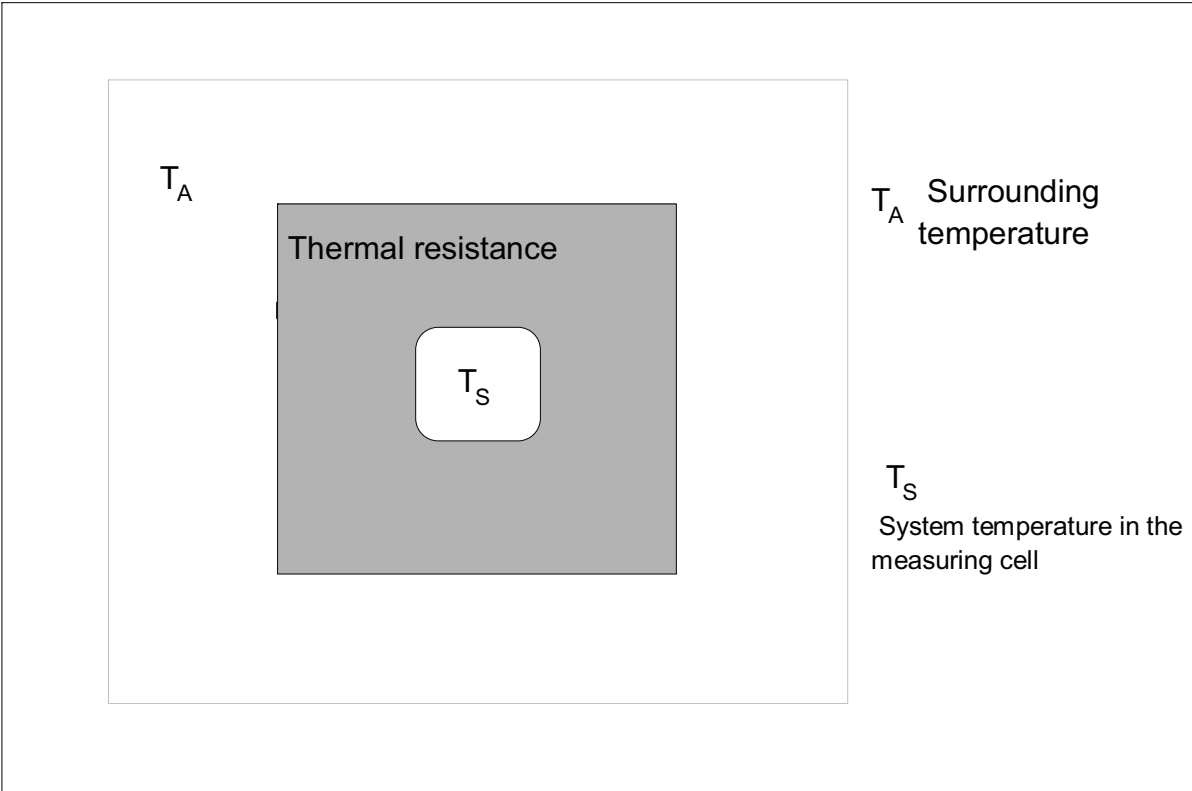
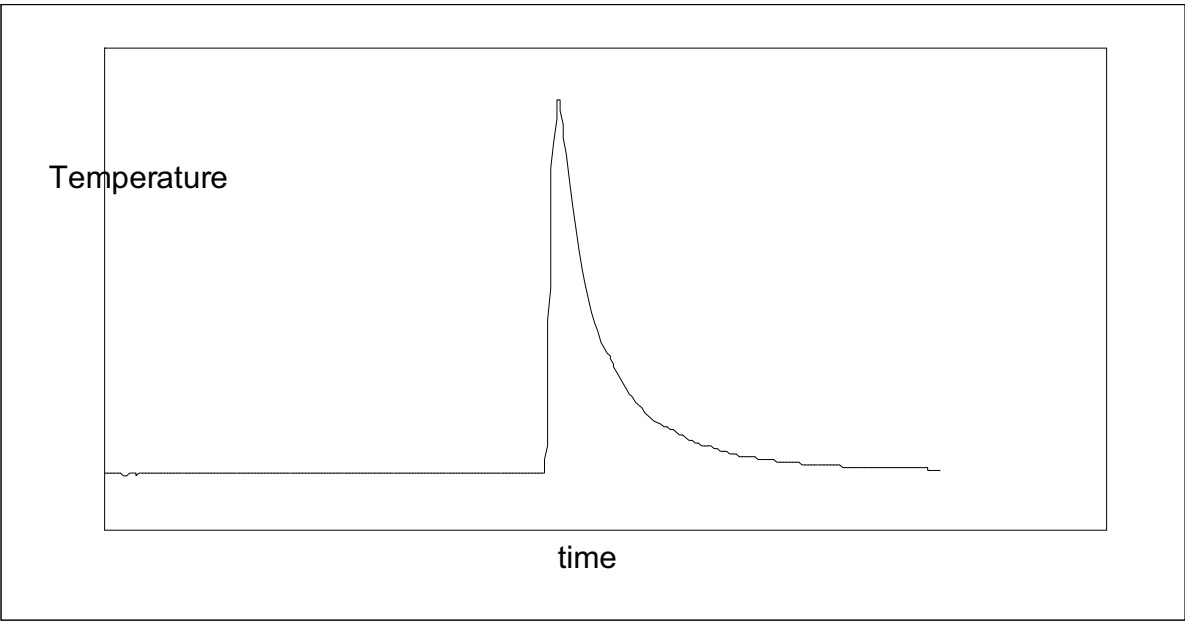Fig. 5. Diagram of the heat conduction calorimeter

Fig. 6. Thermogram obtained by a heat conduction calorimeter

The temperature difference of the thermal resistance is

$$\Delta T = T_C - T_A \tag{4}$$

and at steady state we obtain the relationship

$$\frac{dQ}{dt} = \frac{\Delta T}{R_T} \qquad (5)$$

Integration gives

$$Q = \frac{1}{R_T} \int \Delta T(t)dt \qquad (6)$$

Figure 6 shows the form of a thermogram determined by a heat conduction calorimeter in which the thermal effect generated in the cell appears as a pulse in the curve of temperature versus time. As in the case of isothermal calorimetry, the heat flows to the surroundings, and the change in system conditions can be detected by means of a property that is proportional to heat flow, producing a continuous variation in this case. Measuring the sensor system properties as a function of time and through calibration experiments can determine the amount of heat generated by that system.

3. Adsorption calorimetry

Heats of adsorption of pure gases, which are usually obtained from isotherms using the Clapeyron equation, are unreliable unless extra precautions are taken to ensure reversibility and reproducibility. The calculation of heats of adsorption for mixtures from extensions of the Clapeyron equation is impractical. However, we have recently demonstrated that both adsorption isotherms and multicomponent heats of adsorption can be measured accurately and quickly in a single, inexpensive (Sharma et al., 1994; Spiewak et al., 1994; Dunne et al., 1997; García et al,2008). This paper summarizes the design criteria and construction of our combined calorimetric-volumetric apparatus in sufficient detail to reproduce our instrument, with numerous helpful suggestions to avoid some of the pitfalls associated with adsorption calorimetry. The known technology reported in the literature about the calibration systems (Handy et al., 93; Huertemendía et al., 2005) has been used here to evaluate the results obtained in this work.

3.1 Theory
The isosteric heat of adsorption is defined as the difference between the partial molar enthalpies in the gas and adsorbed phases:

$$Q_{st} = \overline{h}^g - \overline{h}^{\mathbf{a}} \qquad (7)$$

Thus, Q_{st} is the heat of desorption. Even though it is not a heat but the difference of two state functions, the name is well established. The actual heat measured in a particular calorimeter must be related to the thermodynamic definition of isosteric heat in eq 7.

3.2 Idealized calorimeter
An idealized batch calorimeter consists of a dosing cell, a sample cell and a valve between the two, completely enclosed in an isothermal calorimeter at temperature T_0. At the start, the valve is closed, both cells are at temperature T_0, the pressure in the dosing loop is Pd, and the pressure in the sample cell is Pc, with $Pd > Pc$.

When the value is opened, an amount of gas expands from the dosing cell into the sample cell and a portion of this amount adsorbs. The total energy is:

$$U = U^g + U^a = u^g n^g + u^a n^a \qquad (8)$$

The total energy *U should include* contributions from the adsorbent, the walls of the sample cell and dosing cell, and the valve.

However, since the temperature is fixed at T_0, these energies are omitted from eq 8 because they are constant and do not contribute to the change in energy. The total amount of gas in both cells is *ng*. The differential of the total energy is:

$$dU = u^g \, dn^g + n^g \, du^g + u^a \, dn^a + n^a \, du^a \qquad (9)$$

where *dU* refers to the differential energy change after attainment of adsorption equilibrium. Because the temperature is T_0 before and after adsorption, *dug*= 0 and

$$dU = u^g \, dn^g + u^a \, dn^a + n^a \, du^a \qquad (10)$$

The mass balance is:

$$n^g + n^a = cons \tan t \qquad (11)$$

so

$$dn^g = -dn^a \qquad (12)$$

Substituting eq 12 into eq 10:

$$dU = -u^g \, dn^a + u^a \, dn^a + n^a \, du^a \qquad (13)$$

The first law for the combined closed system consisting of the dosing cell, the sample cell and the valve is

$$dU = dQ \qquad (14)$$

where d*Q* is the heat adsorbed by the combined system. For adsorption, d*Q* is a negative quantity. Combining eqs 13 and 14 we obtain

$$-dQ = u^g \, dn^a - u^a \, dn^a - n^a \, du^a \qquad (15)$$

or

$$-\frac{dQ}{dn^a} = u^g - \left[u^a + n^a \frac{du^a}{dn^a} \right] \qquad (16)$$

Because *ha* ≈ *ua* and *hg* = *ug* + zRT_0, comparison of eqs 7 and 16 gives

$$Q_{st} = -\frac{dQ}{dn^a} + zRT_0 \qquad (17)$$

This result was derived by Hill. The first term is the differential heat measured by the idealized calorimeter, and the second term is the difference between the enthalpy and the internal energy in the equilibrium gas phase. $z=PV/RT$, the compressibility factor in the gas phase, is close to unity for sub atmospheric measurements of isosteric heat. The RT_0 term at 25 °C is 2.5 kJ/mol, and typical isosteric heats of adsorption are in the range 10-50 kJ/mol (O´Neil et al., 85).

3.2.1 Thermopiles theory
The Seebeck effect
If two semiconductors a and b are joined together at the hot point and a temperature difference ∆T is maintained between this point and the cold point, see Figure 6(a), then an open circuit voltage ∆V is developed between the leads at the cold point. This effect, called the Seebeck effect after its discoverer T. J. Seebeck (1770 - 1831), can be mathematically expressed by

$$\Delta V = \alpha_s \Delta T \tag{18}$$

here a_s is the Seebeck coefficient expressed in V/K (or more commonly in μV/K). It was found that only a combination of two different materials, a so-called thermocouple, exhibits the Seebeck effect. For two leads of the same material no Seebeck effect is shown, for reasons of symmetry. It is, however, somehow present because the Seebeck effect is a bulk property and does not depend on a specific arrangement of the leads or the material, nor on a specific way of joining them. This bulk property can be expressed as

$$VE_F / q = \alpha_s VT \tag{19}$$

where E_F is the Fermi energy (and $E_F/q = \Phi F$ is the electrochemical potential), and where the Seebeck coefficient αs depends, among other things, upon the chemical composition of the material and upon the temperature.
The Seebeck coefficient of, for example, silicon, can be derived by setting αs as (see Figure 6(b))

$$\alpha_s = \frac{d}{q \, dT}(E_F) \tag{20}$$

For non-degenerate silicon the Seebeck coefficient may be approximated by using simple Maxwell- Boltzmann statistics. Three main effects are present.
First, with increasing temperature the silicon becomes more intrinsic:

$$\frac{d}{q \, dT}(E_F) \bigg|_{E_C - E_F} = -\frac{\kappa}{q}\left(\ln(N_c / n) + \frac{3}{2}\right) \tag{21}$$

where E_c is the conduction-band edge energy, N_c the conduction-band density of states, n the electron density (fixed by the doping concentration) n_d and k the Boltzmann constant.
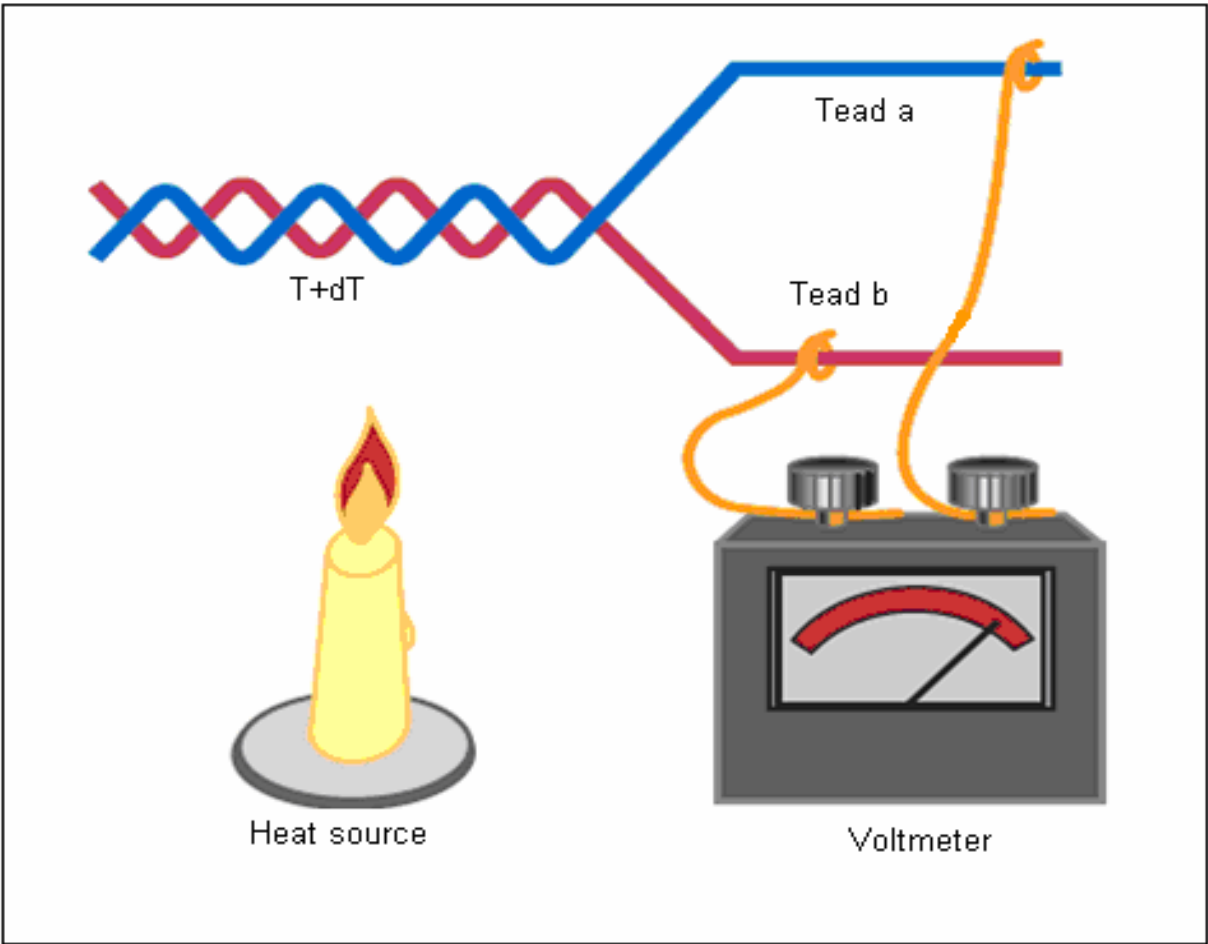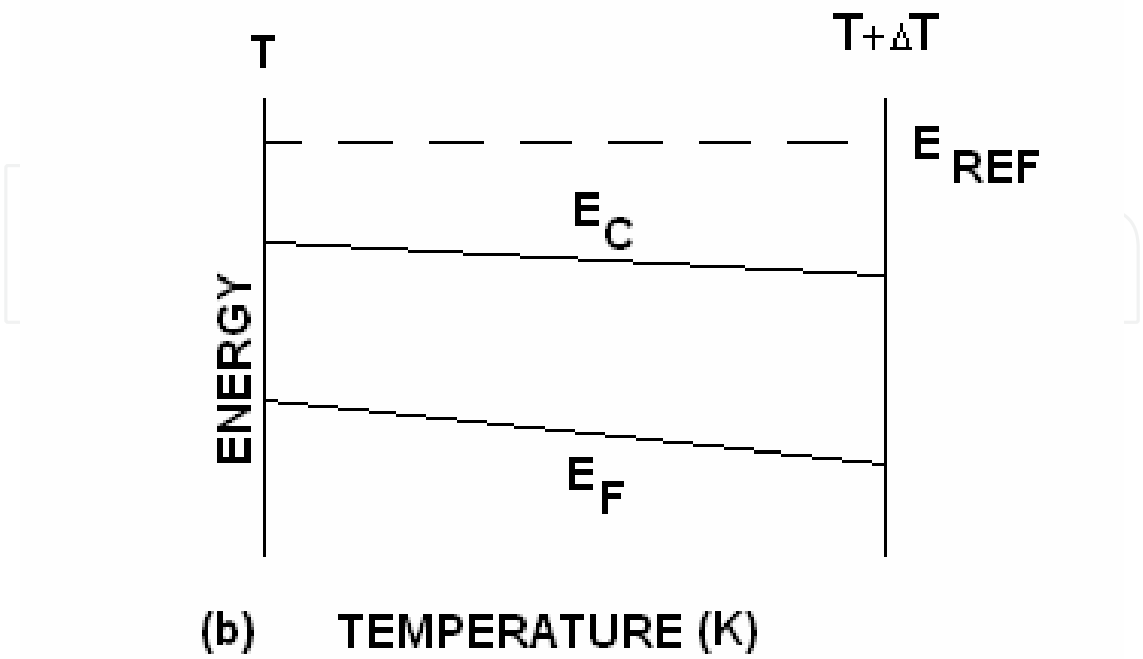
Fig. 6a. Seebeck Efect

Fig. 6b. Variation of E_F due to ΔT

Secondly, with increasing temperature the charge carriers have a higher average velocity, leading to charge build-up on the cold side of the silicon.

Moreover, the scattering of charge carriers is usually energy (and thus temperature) dependent, likewise leading to charge build-up on the cold or hot side of the silicon, depending on whether the hot carriers can move more freely than the cold carriers or are 'trapped' by increased scattering:

$$\frac{d}{q\,dT}(E_F)_\tau = -\frac{\kappa}{q}(1+s)$$ (22)

where τ is the relaxation time (mean free time between collisions) and s is the exponent describing the relation between τ and the charge-carrier energy.

Finally, the temperature difference in the silicon causes a net flow of phonons from hot to cold. In a certain temperature region (-10 - 500 K) and for non-degenerate silicon, a transfer of momentum from acoustic phonons to the charge carriers can occur. As there is a net phonon momentum directed from hot to cold, this will drag the charge carriers towards the cold side of the silicon. This effect may be represented by:

$$\frac{d}{q\,dT}(E_F)_{\phi_n} = -\frac{\kappa}{q}\phi_n$$ (23)

in which Φ_n denotes the phonon drag effect. In sum, the total Seebeck coefficient in non-degenerate silicon becomes:

$$\alpha_s = -\frac{\kappa}{q}\left\{\ln(N_c/n)+\frac{5}{2}+s_n+\phi_n\right\} \quad n-type$$ (24)

$$\alpha_s = +\frac{\kappa}{q}\left\{\ln(N_v/p)+\frac{5}{2}+s_p+\phi_p\right\} \quad p-type$$ (25)

where s is of the order -1 to 2, and where he phonon-drag contribution Φ ranges from 0, for highly-doped silicon, to approximately 5, for low-doped silicon, at 300 K, while Φ ranges from 0, for highly-doped silicon, to 100, for low-doped silicon, at low temperature (100K). In practice, the Seebeck coefficient may be approximated, for the range of interest for use in sensors and at room temperature, as a function of electrical resistivity:

$$\alpha_s = \frac{m\kappa}{q}\ln(p/p_o)$$ (26)

3.3 Experimental
3.3.1 Design criteria
The desired equilibrium information for adsorbed mixtures is the pressure and composition of the gas phase above the adsorbent for a given loading, as well as the heat evolved for differential increases in the loading. Because we considered direct calorimetric measurements of differential heats to be more reliable than differentiation of isotherms at various temperatures, the instrument was built around a Tian-Calvet calorimeter. Practical limitations on the ability to integrate the heat flow in the calorimeter as a function of time

required that equilibrium be established in 15 min or less. The necessity of establishing equilibrium within 15 min of changing the sample loading placed a stringent limitation on the design. The major limitation for the attainment of adsorption equilibrium is gas-phase mixing in the region above the sample. On the basis of a typical gas-phase diffusion coefficient of 0.1 cm²s⁻¹, a tube length of even 10 cm will result in mixing times of 1000 s. This imposes significant challenges on the instrument design. While imposed circulation would alleviate this problem, forced flow would also complicate the design of the calorimeter because of convective heat losses. The maximum distance within our equipment (from the bottom of the sample cell to the diaphragm of the pressure transducer) was approximately 10 cm. The pressure transducer was chosen for its small dead volume. The leak valve for the composition measurements was welded directly on the top of the cell to minimize the dimensions of the apparatus. These design criteria could only be met by a custom-made calorimeter. In general this calorimeter is based in literature design and experience of our laboratory (Giraldo et al., 98)

3.3.2 Practical calorimeter

In the idealized calorimeter, the temperature of the gas in the sample loop decreases upon expansion while the temperature of the gas in the sample cell increases as it is compressed by the incoming gas. In the absence of adsorption, heat is absorbed by the dosing loop and heat is liberated by the sample cell until the pressures equalize and the temperature returns to T_0. For a perfect gas, the two effects cancel because the enthalpy of a perfect gas is a function only of temperature.

Our design is a modification of the idealized calorimeter in which only the sample cell is placed in the calorimeter. Because the dosing loop and valve are external to the calorimeter, adding a dose of gas to the sample cell generates an exothermic heat of compression in the sample cell which is not cancelled by absorption of heat in the dosing loop. The spurious heat of compression calculated from eq 21 is subtracted from the total heat registered by the calorimeter in order to obtain the heat of adsorption.

3.3.3 Description of the Instrument

A diagram of the calorimeter apparatus is shown in Figure 7, the components are described in Table 1. A picture of the sample cell and its connections is shown in Figure 8. The stainless steel cube is the sample cell for the adsorbent and adsorbate. The use of stainless steel to maximize heat conduction through the top of the cell is a crucial element of the design. The stainless cube is surrounded on all four sides and on the bottom by square thermal flow meters (show in the picture) obtained from the Melcor Corporation™. Each thermopile is a 40x40x2 mm ceramic plate with about 240 embedded thermocouples for detecting temperature differences across the plate.

The signal from these thermopiles was input to a data acquisition system with a computer.

The sample cell slides into cubical holes cut into an aluminum block (10x13x8 cm, mass 1 kg). A silicone based heat-sink compound was used to ensure good thermal contact between the Al block and the thermopiles and between the thermopiles and the stainless steel.

The cubic stainless steel cell shown in Figure 8 (on the top) was inserted into a Cajon fitting, which provides a vacuum seal by compression of a Viton O-ring. The Cajon fitting connects to a custom-made T connection onto which the leak valve, the pressure head, the connection to vacuum and the 0.01-in. bore tube from the dosing loop are welded. The leak valve is

connected through a 1/4-in.-o.d. stainless-steel tube; the pressure head is connected through a 1/4-in. δ NPT fitting; the valve that opens to vacuum is connected through a 1/4-in. VCR fitting. The pressure head was chosen for its small dead space (2.0 cm^3). The total dead space is 17.8 cm^3 for the (empty) sample cell, the dead space inside the pressure head, the lines to vacuum, the dosing loop and the RGA leak valve.

No.	Description	Model No.
1	Gas 1 inlet	
2	Gas 2 inlet	
3	To vacuum pump	
4	Three-way valve	
5	Inlet valve to the dosing loop	
6	Outlet valve from the dosing loop	
7	Pressure transducer for the dosing loop	Teledyne™
8	Liquid nitrogen trap	
9	Valco six-way valve	
10	Calibrated dosing loop (5 cm3)	
11	Variable leak valve	Granville-Phillips 203™
12	Cell outlet valve	
13	Pressure transducer for the cell	Edwards™, 655 and 622
14	Reference cell	
15	Calorimeter cell	
16	K-type thermocouple	
17	Thermopiles	Tellurex Corporation™
18	Heat sink (aluminium block)	
19	Mass spectrometer (RGA)	HP GC/MS 5890 series II 5972 MDS
20	Turbopump	Pfeiffer ™
21	Data acquisition board	
22	Computer	

Table 1. Components of microcalorimeter. Key to figure 1

Gas was introduced to the sample cell from the dosing loop using a six-port Valco sampling valve connected to a small bore (0.01-in.-i.d.) tube. The small diameter of the tube prevents back mixing of the mixture into the dosing loop. This tube enters the T-shaped connector from the back (the welded connection does not appear on Figure 3) and extends downward, with the opening 5 cm above the bottom of the sample cell. Two small metal cylinders with a Viton O-ring between them were inserted in the NPT connection to the pressure head to make a vacuum seal.
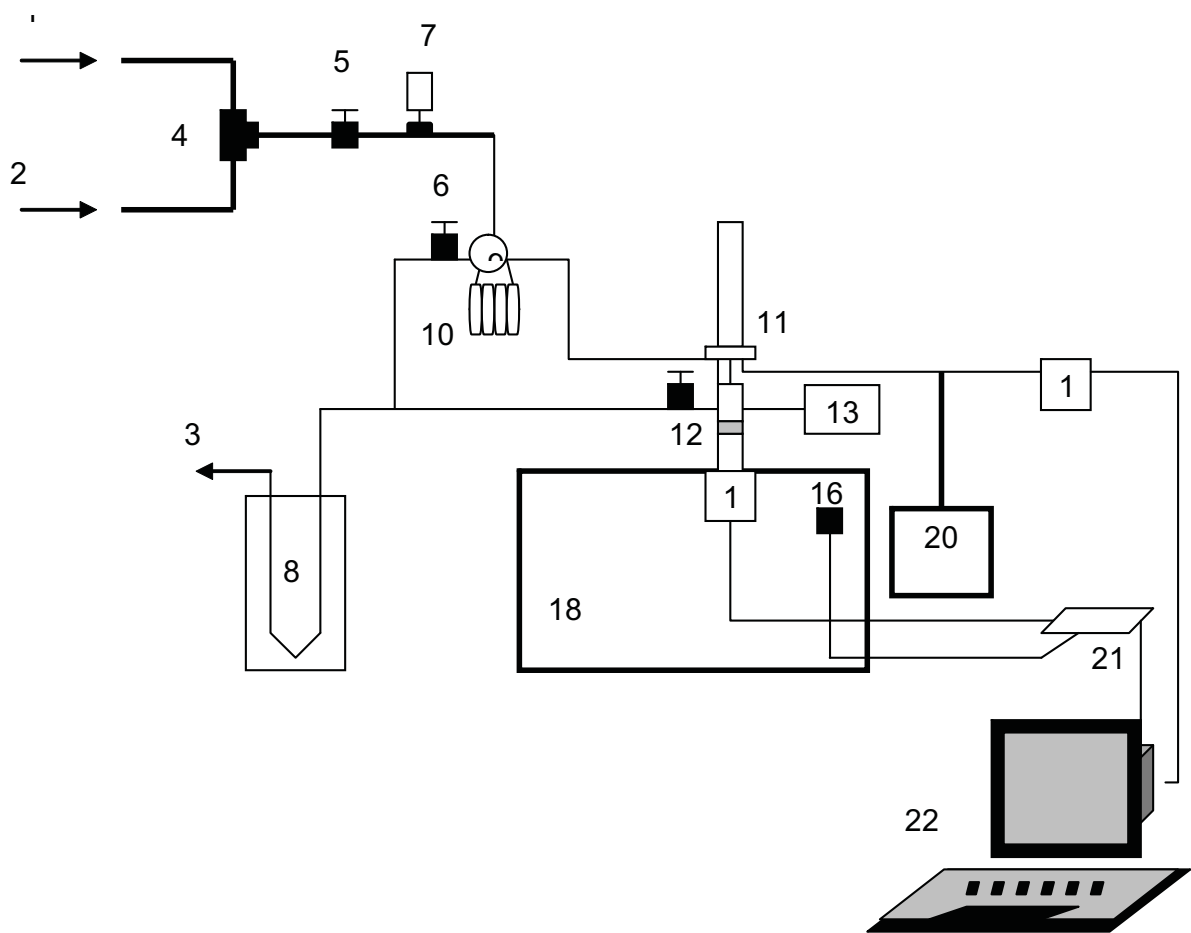
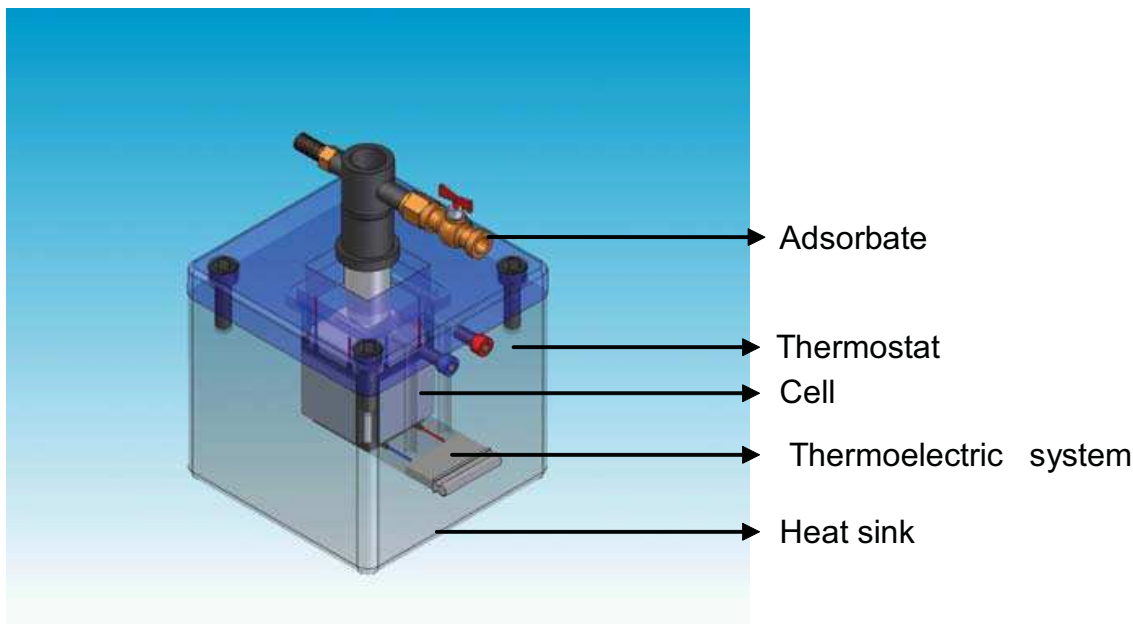Fig. 7. Schematic diagram of microcalorimeter system and auxiliary equipment

Fig. 8. Picture of the stainless steel sample cell and connections to the pressure head, vacuum line, dosing loop and leak valve. The stainless steel sample cell is surrounded by thermopiles set into an aluminum heat sink

The adsorbent was covered with a 1.5 cm layer of glass chips to minimize heat loss through the top of the cell and regenerated in situ.

3.3.4 Electric calibration of the adsorption micro calorimeter.

To establish the correct operation of the micro calorimeter prior to connecting it to the volumetric adsorption unit, we evaluated its sensitivity by determining the calorimeter constant.

The calibration constant gives the voltage generated by the calorimeter when a given amount of heat is emitted from inside the microcalorimetric cell.

There are two methods to determine the calibration constant (K):

Determination of the calibration constant by application of electric power.

This method is based on the dissipation of electric work (W_e) by an electric resistor through which an electric current (i) passes for a certain amount of time (t). This generates a voltage (V_t) in the micro calorimeter and this is measured.

The micro calorimeter calibration constant (K) is given by:

$$K = \frac{We}{\int V_t dt} = \frac{V_c it}{\int V_t dt} \tag{27}$$

Where V_c is the voltage applied to the resistor, i is the current that passes through it, and t is the time expressed in seconds.

Determination of the constant by the stationary state method.

This is an alternate method to the one above, which is useful to compare and evaluate whether the constant (K) assessed by the above method is correct. The method consists on applying a constant voltage (V_c) through the micro calorimeter electric resistor until the voltage generated by the calorimeter (V_t) reaches the condition of stationary state. Under these conditions, K is given by:

$$K = \left(\frac{V_c i}{V_t} \right)_{stationary} \tag{28}$$

3.3.5 Spurious heat of compression in sample cell

Before taking a measurement, the dosing loop and the sample cell are both at the temperature T_0 of the experiment; the pressure inside the sample cell is P_c, and the pressure in the dosing loop is some higher pressure P_d. Increments of gas are added to the sample cell by opening the valve between the dosing loop and the cell.

The temperature of the gas inside the dosing loop falls because of the expansion, while the temperature of the gas inside the sample cell rises as it is compressed by the incoming gas. The calorimeter measures both the latent heat of adsorption and the sensible heat liberated by the compressed gas as it cools to the temperature of the calorimeter. This sensible heat must be subtracted from the heat registered by the thermopiles to obtain the heat of adsorption.

The spurious heat term generated by compression of the gas inside the cell was determined by expanding gas from the dosing loop into a sample cell containing no adsorbent. For a 10 cm³ dosing loop and for a dead space of 18 cm³ in the sample cell, the linear correlation

$$Q_{sp} = a \, \Delta \mathbf{P}$$

(29)

for the experimental data shown in Figure 9 yields a = 4.42 x10-4 J/Torr. ΔP is the driving force for the irreversible expansion: the pressure difference between the dosing loop and the sample cell.

The correlation ignores the effect of adsorption as gas enters the sample cell. For the case of weak adsorption, when only a small fraction of the gas entering the sample cell actually adsorbs, the approximation is justified.

For the case of strong adsorption, when most of the gas entering the sample cell adsorbs, the spurious heat of compression is negligible compared to the heat of adsorption.

Thus, for strong adsorption (95% of gas dose adsorbs) or weak adsorption (5% of gas dose adsorbs), the approximation of considering that the heat of compression is independent of adsorption is acceptable. We have no proof that the correction for the spurious heat of compression is negligible in the intermediate case when about 50% of the gas dose adsorbs, but the excellent agreement of both strong and weakly adsorbing gases with the Clapeyron equation is indirect evidence that eq 29 is adequate for both strongly and weakly adsorbing gases.
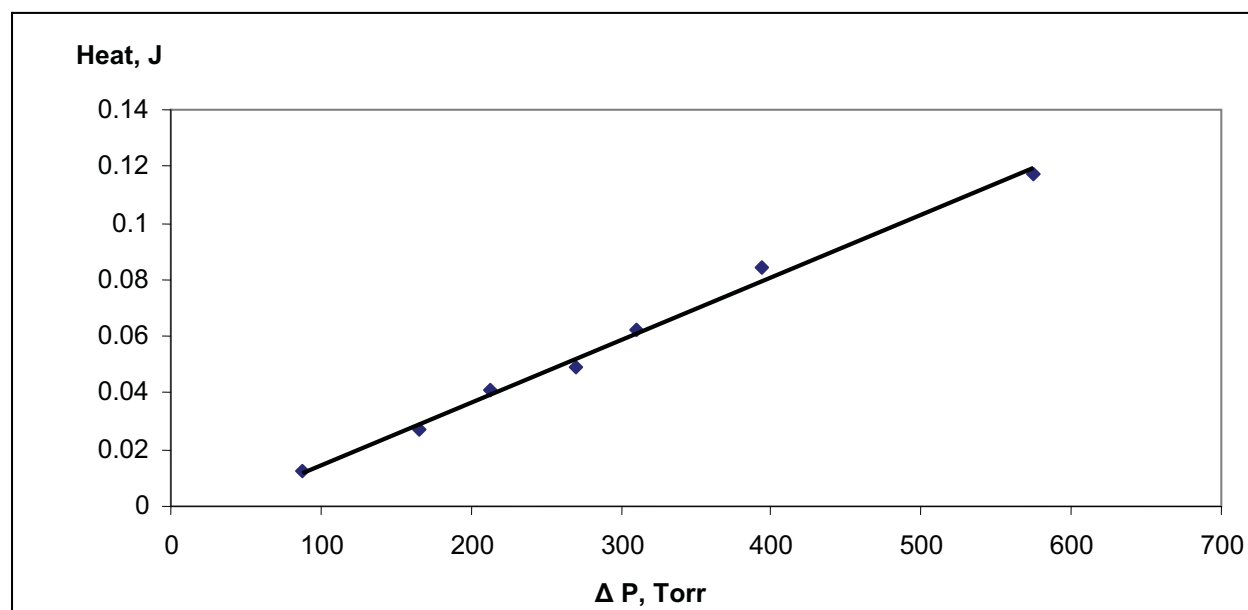

Fig. 9. Linear correlation for a spurious sensible heat term in adding a dose of gas. The difference is the pressure in the dosing loop minus the pressure in the sample cell before opening the valve

Other calorimeters are designed for isothermal introduction of gas to the sample cell. This is accomplished by adding increments of gas slowly through a needle valve so that the temperature of the gas in the dosing loop is equal to the temperature in the sample cell (T_0). In the absence of adsorption, the reversible isothermal introduction of a gas sample generates an exothermic heat inside the sample cell equal to RT_0 per mole of gas added; the signal for this spurious heat term can be eliminated by adding the same amount of gas to a reference cell wired in reverse polarity. Isothermal dosing is effective for the measurement of heats of adsorption of pure gases. For mixtures, the fast, irreversible addition of increments of gas shortens the time required for mixing and equilibration.

3.3.6 Verification of adsorption equilibrium

The mixing time required when a new dose of gas is added to the sample cell containing a gaseous mixture but no adsorbent is about 15 min. Sampling the gas phase continuously to check for equilibrium is impracticable because the amount of gas sampled over 30 min would affect the mass balance used to calculate the amount adsorbed.
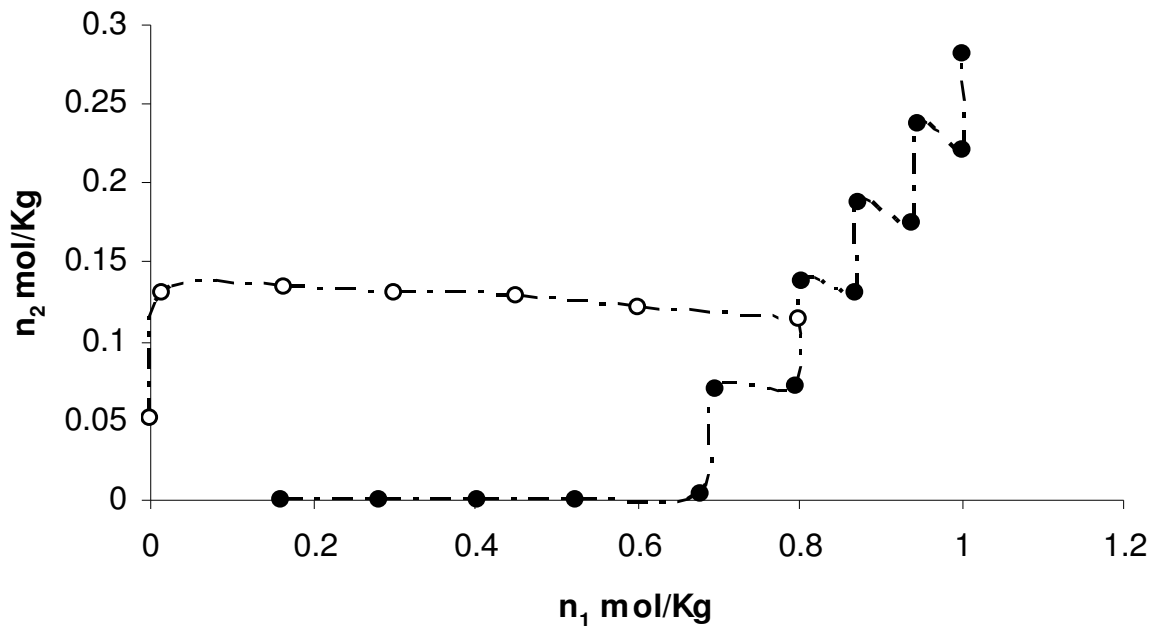
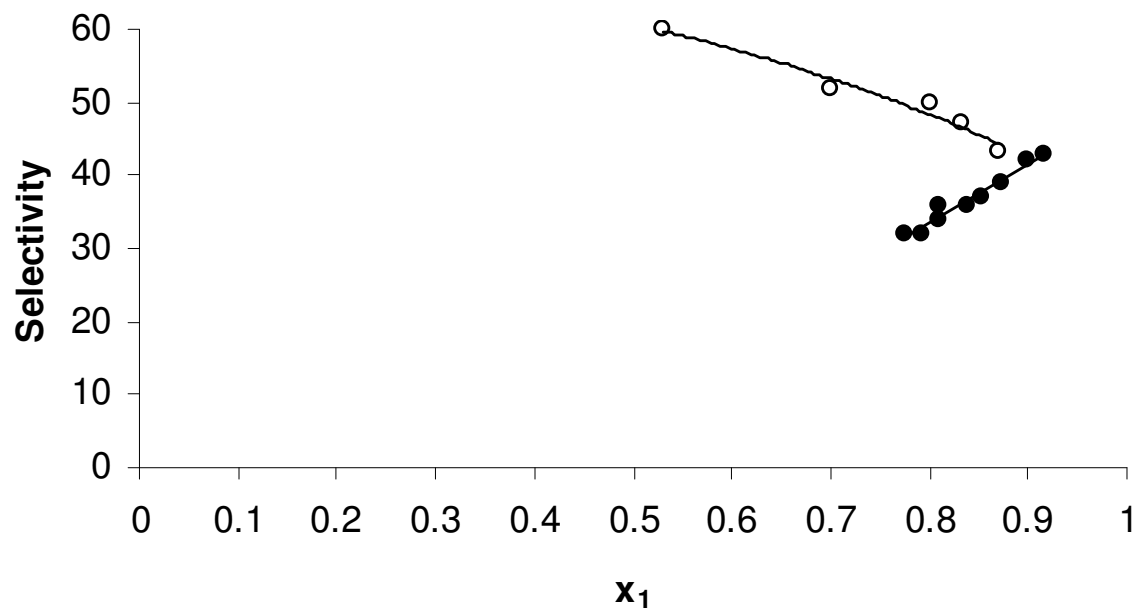Fig. 10. Adsorption of mixtures of SF_6 and CH_4

Fig. 11. Selectivity of SF_6 relative to CH_4 at 24,5 °C. symbols are the same as those in figure 5

Two methods were used to verify the attainment of equilibrium for mixture adsorption. The first method is to fit the experimental data to a model which is thermodynamically

consistent; agreement of the model with the experimental data is an indirect but robust method of verifying equilibration. A second, direct method is to verify that a particular point is independent of the path to reach that point. Figure 10 shows an example for the adsorption of mixtures of SF_6 (component 1) and CH_4 (component 2). The closed and open circles indicate two paths from zero loading to point A; the arrows show the direction of the paths. These two paths intersect at n_1= 0.78 and n_2 = 0.12, or a mole fraction x_1 = 0.87. Figure 11 shows the selectivity for the same two paths; the selectivity curves intersect at x_1 = 0.89. Therefore, within an uncertainty of about 1%, the selectivity is independent of the path followed by the system. There is excellent agreement among them and with values reported in literature (Siperstein et al., 99).

3.3.7 Determination of differential heats from finite doses
The amount dosed Δn must be small enough to measure the differential heat but large enough to generate an accurate heat signal Q. Because the differential heat is defined as the ratio of $Q/\Delta n$ in the limit as Δn goes to zero, the error associated with finite increments needs to be examined.
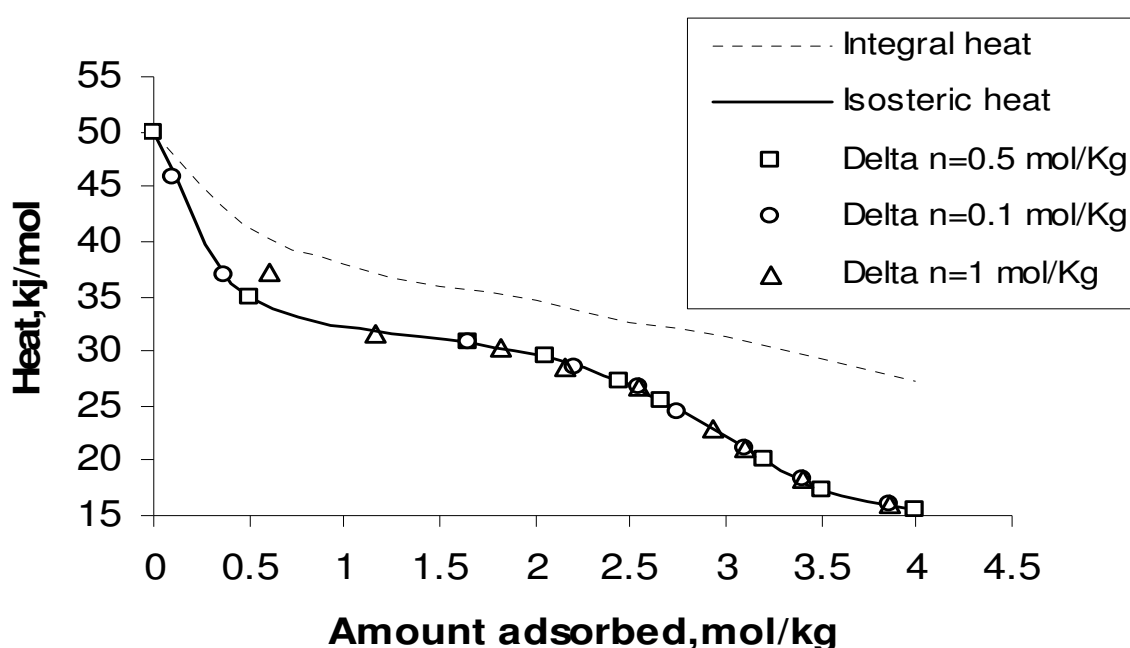

Fig. 12. Comparison of the differential heat of adsorption (solid line) with experimental heats determined with finites doses of gas. The dashed line is the integral heat of adsorption. Heats determined experimentally with small doses of the order 0.12 mol/Kg agree very well with the exact differential heat

Assume that the differential heat $q_d(n)$ is given exactly by the polynomial:

$$q_d(n) = q_0 + d_1n + d_2n^2 + d_3n^3 + ... \tag{30}$$

For a finite amount of gas adsorbed ($\Delta n = n_2 - n_1$), the approximate differential heat qδ measured experimentally is

$$q_\delta = \frac{\int_{n_1}^{n_2} q_d(n)dn}{n_2 - n_1} \tag{31}$$

representing the average value of the differential heat measured at the average loading (n_1 + n_2)/2. Comparison of q_δ with the exact differential heat at the same average loading gives the error:

$$q_\delta - q_d = \frac{d_2}{12}(n_1 - n_2)^2 + \frac{d_3}{8}(n_1 + n_2)(n_1 - n_2)^2 + ... \tag{32}$$

The error is of order of $(n_1 - n_2)^2$. Because the leading term of the error is also proportional to the second derivative of the heat curve, $q_\delta = q_d$ for linear heat curves.

Figure 12 shows hypothetical differential (solid line) and integral (dashed line) heats of adsorption. The points show approximate heats qδ calculated from eq 25 for finite doses n_2 - n_1 = 0.1, 0.5, and 1.0 mol/kg. Only for finite doses as large as 1 mol/kg can the difference between the exact differential q_d and the approximate q_δ be appreciated. Typical experimental values of Δn are of order 0.1 mol/kg. Except for abrupt changes of heat with coverage associated with phase transitions, the error associated with the use of finite doses of gases to measure the differential heat is negligible. There is agreement among them and with values reported in literature (Siperstein et al., 99).

It is convenient to report differential heats of adsorption at the loading n2 instead of the average loading (n_1 + n_2)/2. This introduces errors larger than that predicted by eq 24, especially when the slope of the heat curve is large.

3.3.8 Alternating dosings of each component

Two independent dosings (A and B) are required to measure the individual differential heats of adsorption (q_1 and q_2) from a binary mixture (Siperstein et al., 99) :

$$Q^A = \Delta n_1^A q_1 + \Delta n_2^A q_2 \tag{33}$$

$$Q^B = \Delta n_1^B q_1 + \Delta n_2^B q_2 \tag{34}$$

where Q^A and Q^B are the heats registered by the calorimeter and Δn_1 and Δn_2 are the amounts adsorbed, or desorbed, of components 1 and 2, respectively. When the system of equations (33) and (34) is solved, the individual heats of adsorption are

$$q_1 = \frac{Q^A \Delta n_2^B - Q^B \Delta n_2^A}{\Delta n_1^A \Delta n_2^B - \Delta n_1^B \Delta n_2^A} \tag{35}$$

$$q_2 = \frac{Q^B \Delta n_1^A - Q^A \Delta n_1^B}{\Delta n_1^A \Delta n_2^B - \Delta n_1^B \Delta n_2^A} \tag{36}$$

Dosing of one component generates a positive incremental adsorption of that component which is normally 1 or 2 orders of magnitude larger than the accompanying desorption of the other component. The solution of eqs 27 and 28 requires that the dosing of the components be alternated; successive dosings of the same component generate an indeterminate solution.

4. Experimental results

4.1 Electric calibration of the adsorption micro calorimeter: (by applying electric power)

Table 2 shows the calibration constants obtained for the micro calorimeter operation conditions. Additionally, it presents the values reported at different voltage levels, which range between 12.34 ± 0.12 W V^{-1} and 16.67 ± 0.32 W V^{-1}. These values show the sensitivity of the micro calorimeter built here, which is higher than that of equipments reported in literature and even of those built in our laboratory previously. This constitutes a considerable contribution to the construction of this type of instruments.

Figure 13 shows a typical thermogram obtained with the calorimeter, which corresponds to an electric energy of 1 joule inside the cell, which contains only air. From this type of thermograms the calibration constant (K) can be obtained. It is necessary to point out the great stability of the baseline before and after the thermal effect.

Total electrical energy (J)	Electrical power (mW)	Calibration constant, K (W.V^{-1})*
4.500	25.00	22.21 ± 0.31
3.000	16.00	21.45 ± 0.11
2.000	9.000	23.68 ± 0.06
0.700	4.000	24.25 ± 0.21
0.180	1.000	25.41 ± 0.23
0.045	0.250	22.64 ± 0.14

Table 2. Calibration constants obtained for the micro calorimeter obtained applying a known electrical power
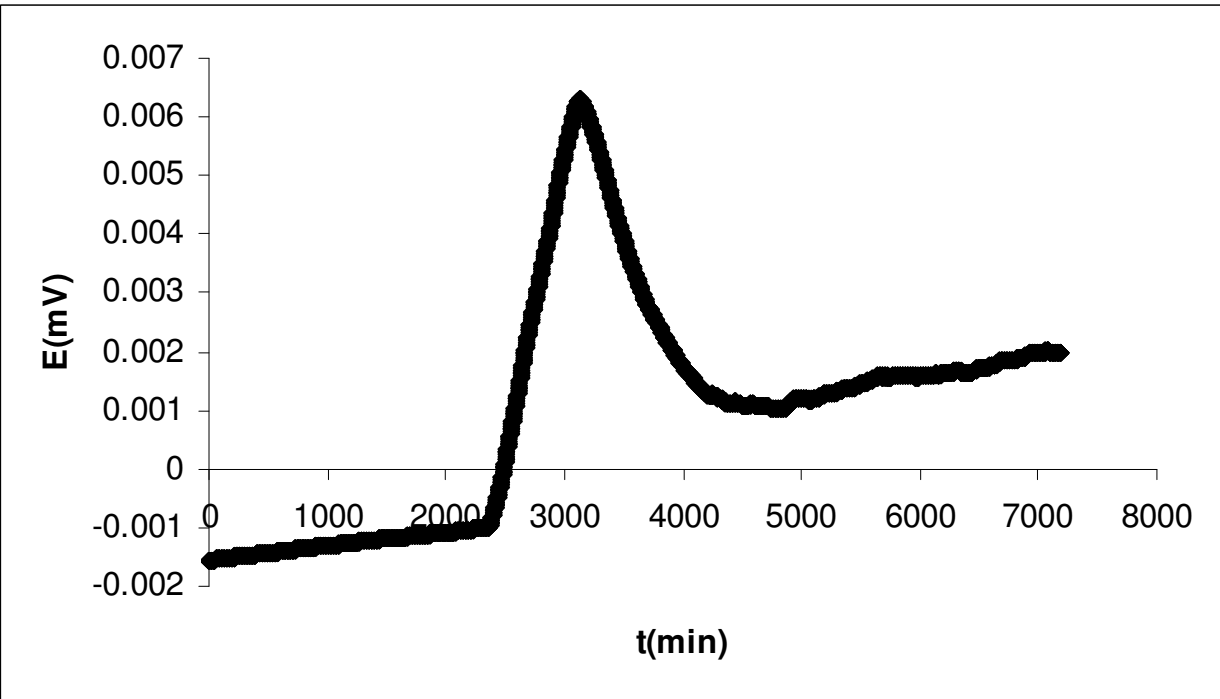

Fig. 13. A typical thermogram of electric calibration by electrical input

4.2 Calibration by stationary state method

Table 3 shows the calibration constants obtained for the equipment built here. These results strongly agree with the previous methodology and with the laboratory previous works.

The voltage signal from the calorimeter was determined as a function of the rate of heat dissipation (dQ/dt) I^2R in a platinum resistance wire wrapped around the outside of the cell in thermal contact with the cell wall and the thermopiles. Similar difficulties were encountered by Handy (Handy et al., 93) the voltage-to-power ratio for a resistor inside the cell was 9% lower than that for an externally wrapped resistance wire. The difference was attributed to heat losses. We chose the Clapeyron equation as the more reliable method of calibration.

Applied voltaje (V)	Electrical power (mW)	Calibration constant, K (W.V^{-1})*
0.254	0.060	24.12 ± 0.31
0.567	0.230	24.15± 0.15
1.009	0.980	23.45 ± 0.64
2.084	3.920	13.23 ± 0.22
3.096	8.860	22.62 ± 0.41
4.084	15.92	23.84 ± 0.45
5.096	24.75	22.22± 0.2

Table 3. Steady state calibration constants obtained for the microcalorimeter

Figure 14 illustrates a thermogram obtained when an electric power of approximately 10mW disperses inside the micro calorimetric cell.

A secondary calibration of the calorimeter (0.045W/V) is based upon the Clapeyron equation applied to a series of adsorption isotherms measured in a separate, high-precision volumetric apparatus for ethane on silicalite (MFI) synthesized in our laboratory. The calibration constant for ethane was confirmed by excellent agreement of calorimetric data with the Clapeyron equation for SF_6, CO_2, and CH_4. The calibration constant is independent of the amount of adsorbent in the cell.

For the presentation of experimental results, it would be helpful that one of the variables, such as the total pressure or fugacity of one of the components, could be held constant.

However, the necessity of alternating doses generates a locus similar to the closed circles shown in Figure 6. The inability to obtain data along some locus, such as an isobar, is annoying but does not affect the analysis of the experimental data for activity coefficients and excess functions. After covering the entire phase diagram for a binary mixture by varying the preloading of the pure components, a model fitting the experimental data can be used to generate loci such as isobars or constant loading of one component.

Figure 7. Comparison of the differential heat of adsorption (solid line) with experimental heats determined with finites doses of gas. The dashed line is the integral heat of adsorption. Heats determined experimentally with small doses of the order 0.12 mol/Kg agree very well with the exact differential heat.

Since our first measurements of heats of adsorption from binary mixtures reported in 1997 for CH_4 and C_2H_6 in silicalite and for CO_2 and C_2H_6 in NaX, we have completed experiments for four other binary mixtures; one of them is reported in this paper (SF_6 and CH_4 on NaX). Presently, we are computing thermodynamic excess properties for these mixtures, especially adsorbed-phase activity coefficients, excess free energy, excess entropy, and heat of mixing in

the adsorbed phase. It is interesting that all of the excess functions are negative: activity coefficients are less than unity, and the heat of mixing is exothermic in every case.
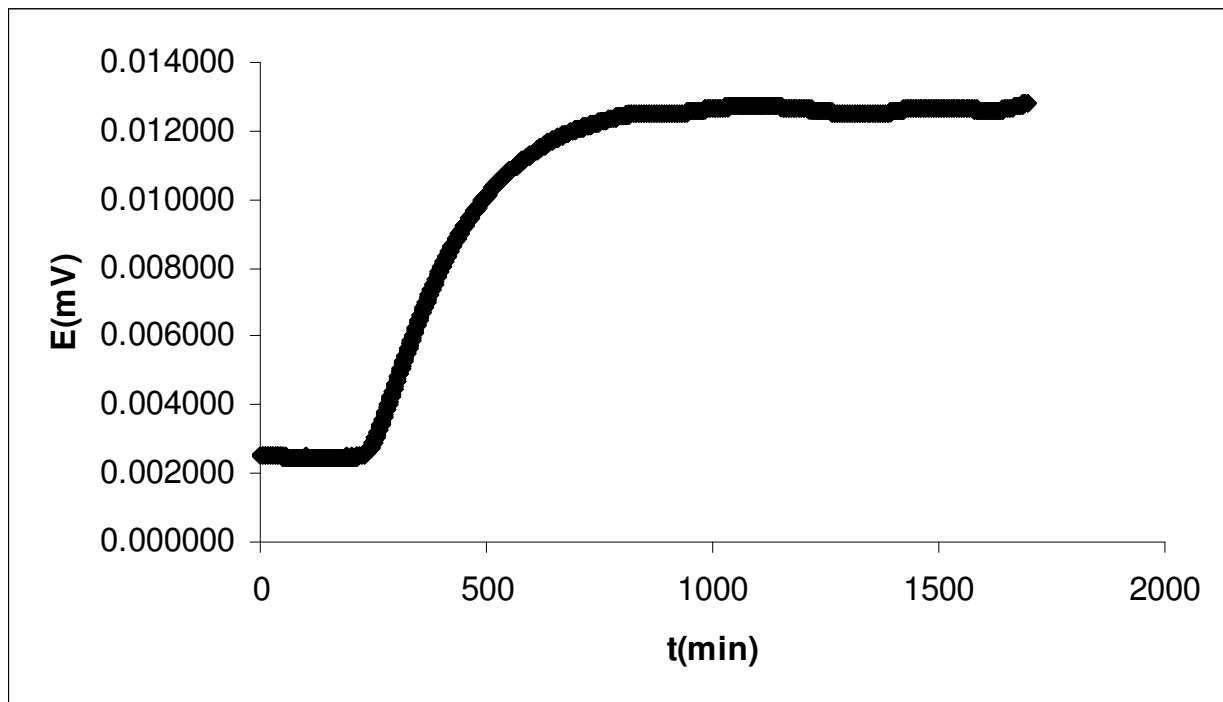

Fig. 14. A typical thermogram of electric calibration by stationary state

5. Variation of the noise levels in the baseline of an adsorption microcalorimeter

To measure precisely the heat, various elements can be used. The thermometer can be very stable, but only by a period of time that exceeds the experiment. However, other sensors can be used, such as termistors that are particularly useful for several reasons: high thermometric sensitivity; built with simple and inexpensive components; and at last, they have a small mass then, the time constant can be also small. The principal disadvantage is that the termistor heats itself. Some electronic circuits are sometimes used when termistors are employed to measure the temperature (Hansen and Hart, 2004), like the modified Wheatstone bridge, one of the most used because of its simplicity, easy operation and high sensitivity. However, when a high sensitive system is required, like in calorimetric studies for the gas-solid interphase, a Calvet-type adsorption calorimeter is the chosen. In these equipments the measure system consists in a group of thermo couples in series that form the thermo battery, which is the measure thermo element. These thermo elements use the Seebeck effect, where a difference in the temperature generates a difference in the potential (Martínez et al., 2004). A thermo battery works very well in theory, but errors are common in practice, which are attributed to small electrical signals generated by the unions, connections and imperfections in the electrical circuit employed in the laboratories to obtain the thermo electrical signal. Within them it can be mentioned: a) the length, thickness, polarity of the terminal wires in the thermo batteries; b) the number of connections in the system; c) the magnitude of the thermal gradients along the wires in the thermal elements. These factors can generate noise levels that could invalidate the calorimetric measures if taken into account that the magnitude of the thermal effect in adsorption

calorimetry, in some cases, are about µW. In this context, it is called noise to every undesired signal that overlaps the genuine signal and it is not directly related to the thermal measure and could distort it. There are three kinds of fundamental noises in every electronic component, two of which are: a) thermal noise or Johnson; b) shot noise.

5.1 Thermal noise or Johnson

Every kind of resistances generates, by themselves and by their terminals, a voltage with random fluctuations like thermal noise or Johnson, which is caused by the charge carrier random movement in conductor materials. It is always produced at temperatures above absolute zero (-273ºC or 0 K).

This kind of noise is related to the no continuous nature of the electrical current, formed by a discrete charges flow that causes statistical fluctuations in the current. The shot noise, as well as the thermal noise, is a kind of white noise.

In this work, we studied the noise signal behavior generated in an adsorption micro calorimeter built in our laboratory, based in others built previously, respect to the applied potent and the temperature, to establish if the noise level can eventually affect the measures in the gas-solid interface (García et al., 2008).

5.2 Experimental

The measures are realized in a micro calorimeter designed in our laboratory, which basic scheme is shown in Figure 15. I consist basically in two parts: a) adsorption part and b) the micro calorimeter itself. Each one of these parts is detailed in the figure.
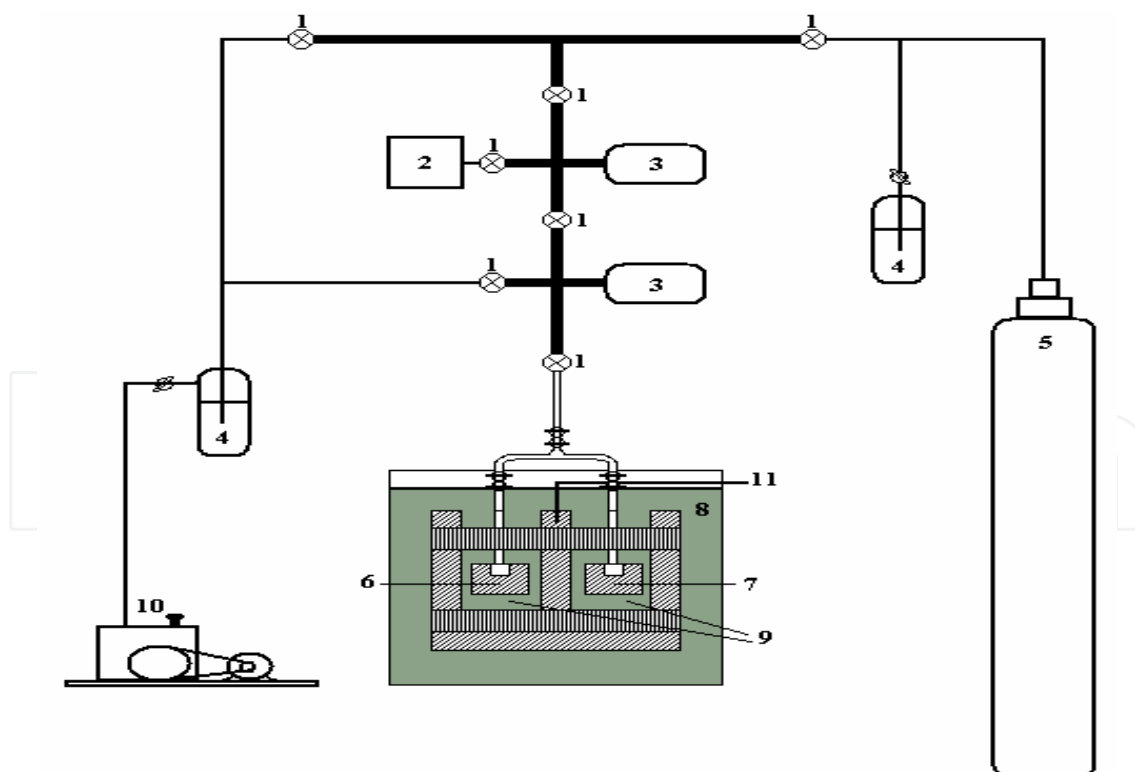

Fig. 15. Adsorption Micro calorimeter
1. Precision Valves 2. Calibration volume or storage. 3. Pressure Transducers. 4. Nitrogenous Traps 5. Adsorbate. 6. Reference Cell. 7. Reaction Cell. 8. Heat Storage. 9. 3D-Type Heat Sensors. 10. Vacuum System. 11. Temperature Control Sensor

A detail of the calorimetric cell is shown in Figure 16. It consists in two calorimetric cells; one of them acts as the reference cell and the other as the measure cell. The 3D-Type heat sensors used are zoomed in the same figure.

The equipment is insolated from the surroundings to control the temperature by a special material with low thermal conductivity. The calorimeter has two resistances with the same magnitude, which value is about 698.32 KΩ. The measurements scheme is shown in Figure 17; it is highlighted with an interrupted line, the external electrical connections between the adsorption micro calorimeter and the data entry system, which contribute to the noise in the signal measurements.
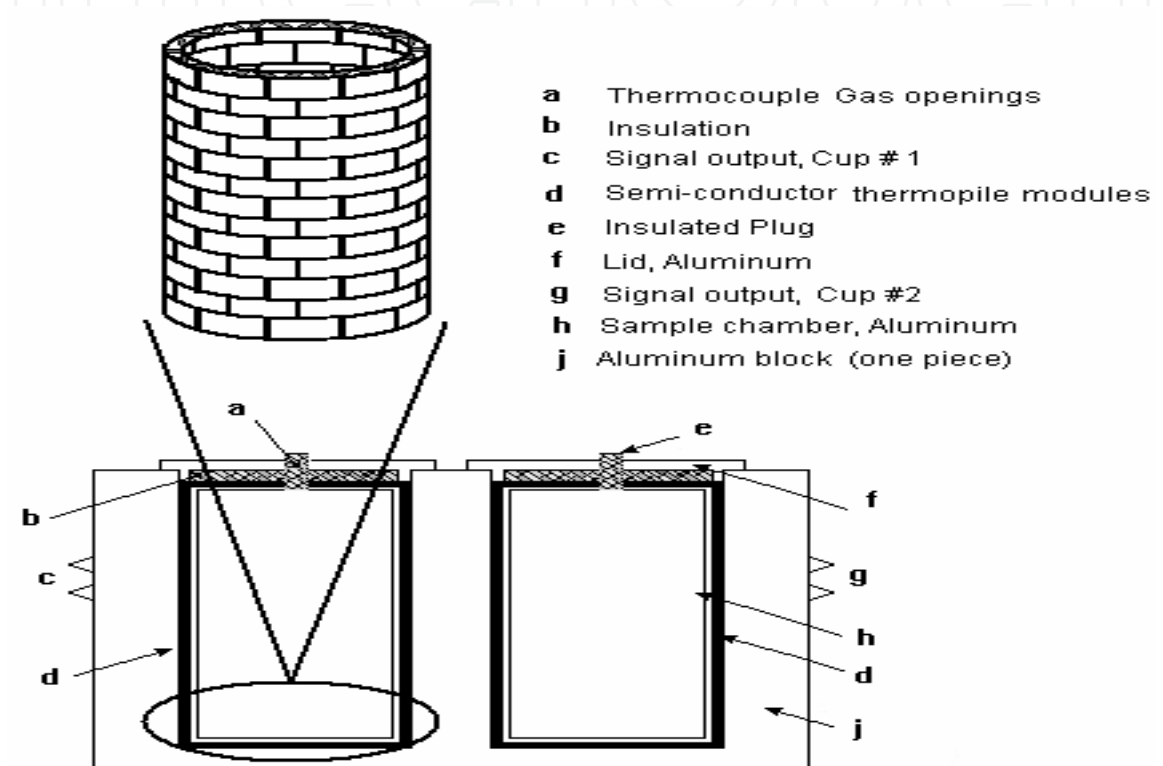
Fig. 16. Calorimetric Cell in the adsorption micro calorimeter
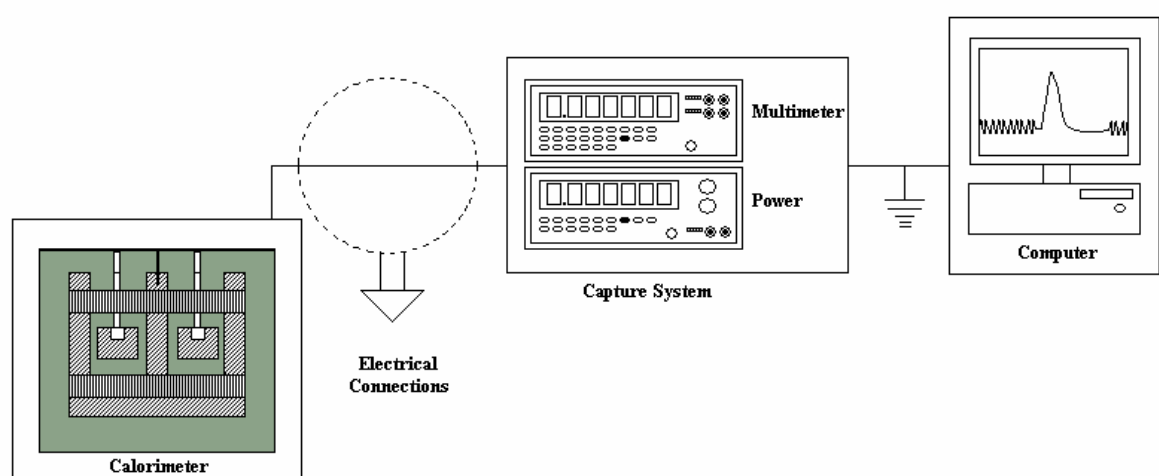
Fig. 17. Sistema de captura de datos

To determine the noise level, different signal potencies are applied by means of the electrical resistance with a fix electrical work at different temperatures and under experimental work conditions in the surroundings. It was also realized some essays at a fix temperature and varying the electrical work level. A highly stabilized source Agilent™ E3649A Al model applies the potential and a multimeter Agilent™ 34401 with 6½ numbers enters the data. This multimeter is connected to a PC by a GPIB interface, where the signals are evaluated.

5.3 Results

The results at a constant temperature of 18ºC, where obtained by putting the system in an air thermostat and varying the applied potential and the electrical work levels. The applied potential varied from 0.40 to 1.5 volts that corresponds to electrical works from 0.19 to 2.70 Jules. Figure 18 shows that increasing the electrical work magnitude, increases the noise level about 10 µV and repeated tests for the lowest values of electrical work increase the noises values about 15 µV. These results are interesting under an experimental point of view in fine calorimetry like adsorption because, independently of this values magnitude, it is important to compare them with the thermal effect magnitude and then, quantify the possible error introduced in the measures. When dissipating a small electrical work, there is a tendency to about 1 µV noise in the baseline; when shooting bigger electrical works, it increases to magnitude orders no too large compared to the measurements.
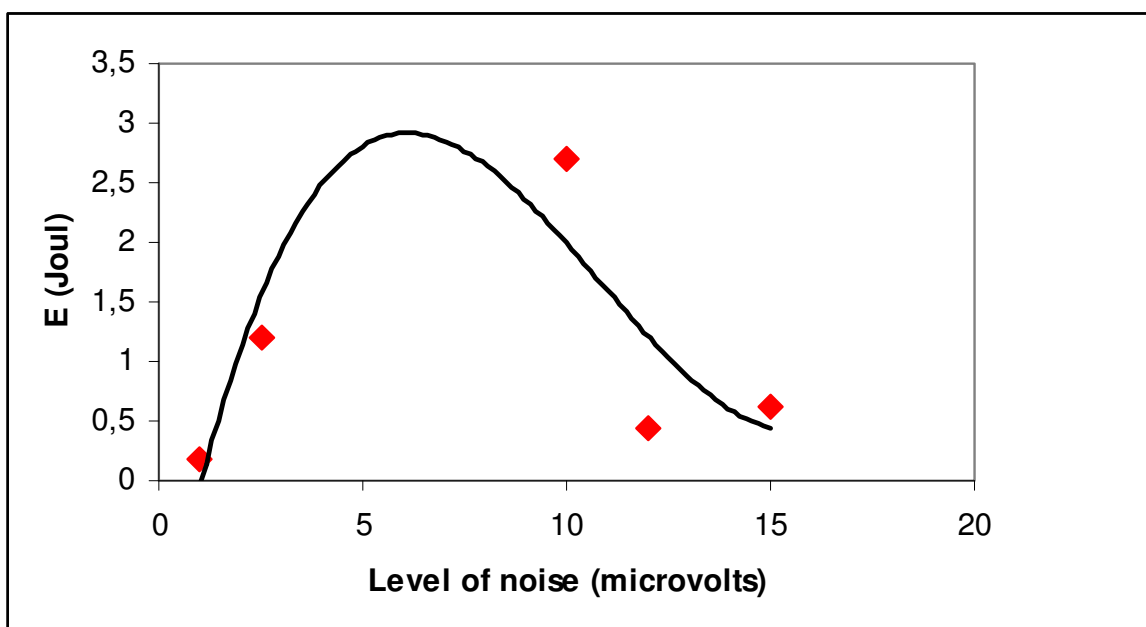

Fig. 18. Peak to Peak Noise Level at 18 °C varying the Voltage Level

Although in specialized bibliography there are some studies about the noise level in calorimeters and/or in calorimetric measurements and different magnitude orders have been reported in different kind of calorimeters (Degroote and García, 2005), this work focuses in the importance of determining in a precise way, the signals that are not associated with what is under measure, like noises, which are due to the connections between the different parts of the equipment.

Figure 19 shows a calibration potenciogram for the constructed calorimeter with a zoom in the baseline signal part; it is clear that the noise level is insignificant respect to the signal, with a noise value in this case of 0.5 µV for a dissipated electrical work of 0.42 Jules.
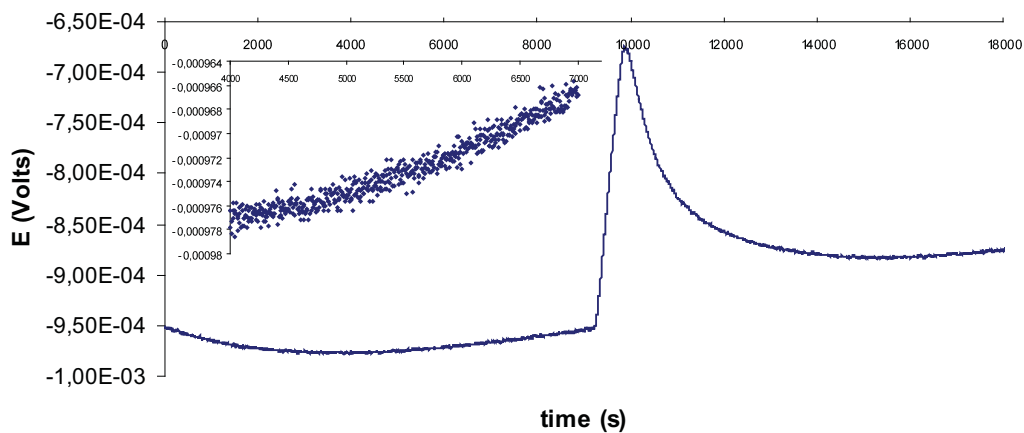

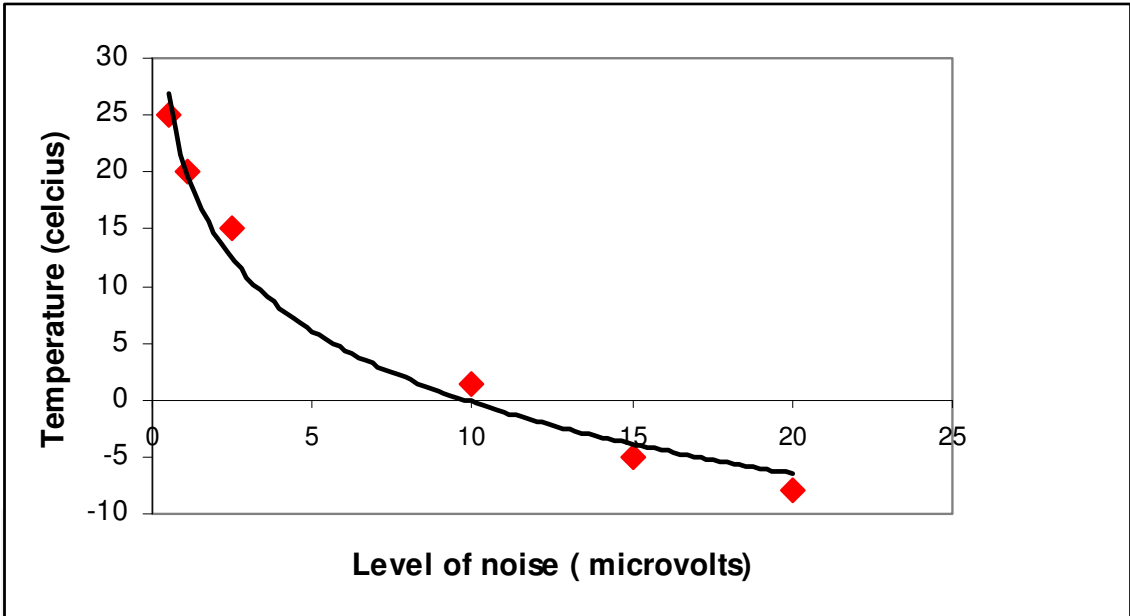Fig. 19. Potenciogram: Applied Work 0.42 Jules; Peak to Peak Noise 0.5

Fig. 20. Peak to Peak Noise Level applying a 0.42 Jules Work

In this work, it was studied if the time constant value (τ) of the equipment could be affected by the noise level magnitude. It was established that it is not true, obtaining repetitive values about 120 seconds, quite similar to commercial equipment like SETARAM™.

Figure 20 shows the behavior of the calorimetric system when is varied the temperature at a fix level of electrical work (0.42 Jules). This essay is realized taking into account that the equipment was designed to work in a temperature range from -196°C to 600°C. The figure shows that near room temperature the signal noise level is about 0.5 µV, which permits without any doubt to carry out experiments with magnitudes about 5 mV with a good precision. At low temperatures the noise level increases up to about 20 µV. It must be taking into account that when the temperature decreases in the calorimeter, a thermal gradient is

generated between the heat sensor terminals inside the calorimeter and the ones connected to its external part, causing a higher noise level in the signal. Certainly, it is observed here the thermal noise or Johnson that is present at temperatures higher than -273ºC, where the connections can be considered resistances that generate by means of their terminals a voltage with random fluctuations. This generates a random movement in the charge carrier in conducting materials. The resistance has a conduction band with electrons free that tends to move freely in any direction, the thermal energy of the surrounding provokes this random movement that at the same time increases the temperature.

In Figure 21 it is shown the noise level monitoring keeping constant the temperature at 18ºC by more than 36 hours.
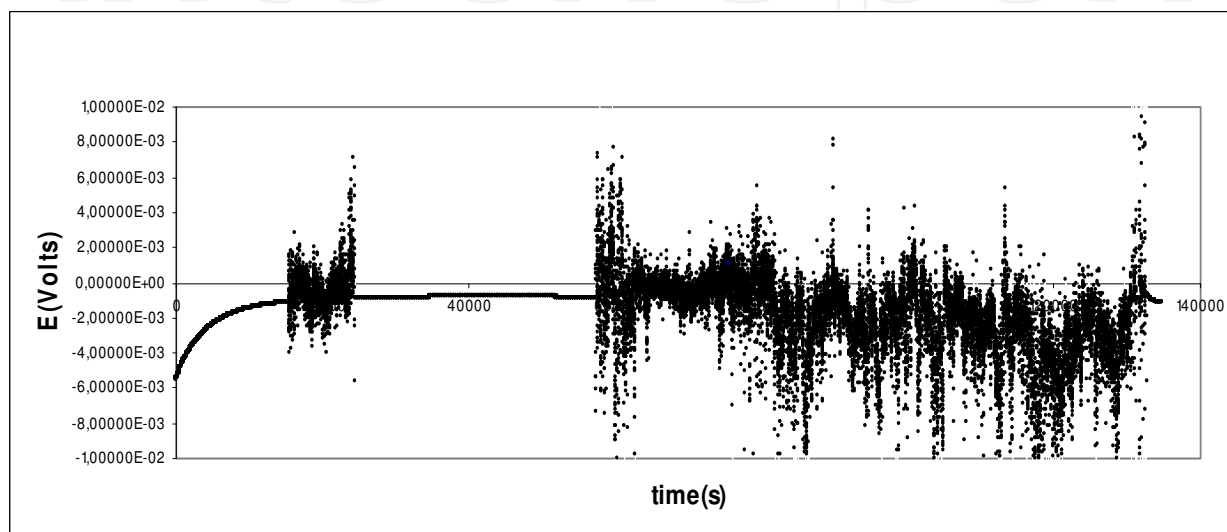

Fig. 21. Noise Signal in the Calorimeter during 36 hours

It is noticed that the stability in the baseline is very important, where the noise level is under 0.5 µV; the scale is zoomed to a better visualization of the noise signal. It is important to recall that the electrical connections generate noises that can also be associated to the shot-type noise.

6. Conclusions

It was built an adsorption micro calorimeter at an affordable price, which is useful to measure adsorption heats and solid surfaces reactions. The equipment works in a temperature range from 77 K to 500 K. It was demonstrated experimentally in this work that it works at 298 K. Calorimetric cells in glass and stainless steel were prepared for the treatment of samples in static form. These cells enable the study of various catalysts in general. The time constants in vacuum and at atmospheric pressure were determined. These constants show that this equipment is useful to study processes with slow kinetic. The sensitiveness of the equipment is high. Finally the noise in the signal is very small and do not affect the measures.

7. References

Armstrong, G.T. (1964). The calorimeter and its influence on the development of chemistry. *J. Chem. Ed.*, 44 (6), 297-307, ISSN 00219584.

Aroua, M.K.; Daud, W.M.A.W.; Yin, C.Y.; Adinata, D. (2008). Adsorption capacities of carbon dioxide, oxygen, nitrogen and methane on carbon molecular basket derived from polyethyleneimine impregnation on microporous palm shell activated carbon. *Separation and Purification Technology*, 62, 609-613, ISSN 13835866

Bastos Neto, M ; Torres, A. E. B. ; Azevedo, D. C. S. ; Cavalcante JR, C. L. (2005a). A Theoretical and Experimental Study of Charge and Discharge Cycles in a Storage Vessel for Adsorbed Natural Gas. *Adsorption-Journal of the International Adsorption Society*, 11, 147-157, ISSN 09295607

Bastos Neto, M ; Torres, A. E. B. ; Azevedo, D. C. S. ; Cavalcante JR, C. L. (2005b). Methane Adsorption Storage Using Microporous Carbons Obtained From Coconut Shells. *Adsorption-Journal of The International Adsorption Society*, 11, 911-915, ISSN 09295607

Belmabkhout, Y.; Sayari, A. (2009). Adsorption of CO_2 from dry gases on MCM-41 silica at ambient temperature and high pressure. 2: Adsorption of CO2/N2, CO2/CH4 and CO2/H2 binary mixtures, *Chemical Engineering Science*, 64, 3729 – 3735, ISSN 00092509

Buckton G. (1995). Application of isothermal microcalorimetry in the pharmaceutical sciences. *Thermochim. Acta*, , 117-125, ISSN 00406031

Degroote, E.; García Ybarra, P.L. (2005). Flame propagation over liquid alcohols Part I. Experimental results *J. Therm. Anal. Cal.*, 80, 541-548, ISSN 14182874

Denoyel, R; Fernandez-Colinas, J.; Grillet, Y.; Rouquerol J. (1993). Assessment of the surface area and microporosity of activated charcoals from immersion calorimetry and nitrogen adsorption data *Langmuir*, 9, 515-518, ISSN 07437463.

Dunne, J.A.; Rao, M.; Sircar, S.; Gorte, R.J.; Myers, A.L. (1997). Calorimetric Heats of Adsorption and Adsorption Isotherms. 3. Mixtures of CH_4 and C_2H_6 in Silicalite and Mixtures of CO_2 and C_2H_6 in NaX. *Langmuir*, 13, 4333-4339, ISSN 07437463.

Figueroa, J. D.; Fout, T.; Plasynski, S.; Mcilvried, H.; Srivastava, R. D. (2008). Advances in CO2 capture technology – The U.S. Department of Energy's Carbon Sequestration Program, *International Journal of Greenhouse Gas Control*, 2, 9-20, ISSN 1750-5836

Garcia-Cuello, V; Moreno-Piraján, J. C.; Giraldo, L.; Sapag, K.; Zgrablich, G. (2009). A new microcalorimeter of adsorption for the determination of differential enthalpies. *Microporous and Mesoporous Materials*, 120, 239–245, ISSN 13871811.

Garcia-Cuello, V; Moreno-Piraján, J. C.; Giraldo, L.; Sapag, K.; Zgrablich, G. (2008). Determination of Differential Enthalpy and Isotherm by Adsorption Calorimetry. *Research Letters in Physical Chemistry*, 5, 4 pages, ISSN 16876873

Giraldo, L.; Moreno, J.C.; Gómez, A. (1994) Construcción de un calorímetro isoperibólico de inmersión de precisión. *Rev. Col. Quim.*, 23, 1-14, 01202804

Giraldo, L.; Moreno, J.C.; Gómez, A. (1996) Instrumentación calorimétrica: calorimetros isoperibolicos y de conduccion de calor. *Revista Química Actualidad y Futuro*, 5, 1996, 90-95, ISSN 01213644

Giraldo, L.; Moreno, J.C.; Gómez, A. (1996) A heat-conduction flow microcalorimeter for solute transfer enthalpy determinations: design and. calibration. *Instrumentation Science & Technology*, 26, 521-530, ISSN 15256030

González, M.T.; Sepúlveda-Escribano, A.; Molina-Sabio, M.; Rodríguez-Reinoso, F. (1995) Correlation between Surface Areas and Micropore Volumes of Activated Carbons Obtained from Physical Adsorption and Immersion Calorimetry. *Langmuir*, 11 , 2151-2155, ISSN 07437463

Gravelle, P.C. (1972) Heat-flow microcalorimetry and its application to heterogeneous Catalysis, *Adv. Catal.*, 22, 191–263, 16154150

Gravelle, P.C. (1985) Aplication of adsorption Calorimetry to the study of heterogeneous catalysis reactions. *Thermochimica Acta*, 96, 365-376, ISSN 00406031

Handy, T.L.; Sharma, S.B.; Spiewak, B.e.; Dumesic, J.A. (1993) A Tian-Calvet heat-flux microcalorimeter for measurement of differential heats of adsorption. *Meas Sci. Technol.*, 4, 1350-1357, ISSN 09570233

Hansen, L.D.; Hart, R.M. (2004) The art of calorimetry. *Thermochim. Acta*, 417, 257-262, ISSN 00406031 .

Hemminger W. and Hohne G. (1984) Calorimetry fundamentals and practice. Ed. Verlag Chemie. Florida.

Hohne, G.W.H.; Hemminger, W.; Flammersheim, H.J. (1996) Differencial Scanning Calorimetry. *An Introduction for practitioners.*1st Edition; Springer; Berlin

Huertemendía, M.; Giraldo, L.; Parra, D.; Moreno, J.C. (2005) Adsorption microcalorimeter and its software: design for the establishment of parameters corresponding to different models of adsorption isotherms. *Instrumentation Science & Technology*, 33, 645-660, ISSN 15256030

Kjems, J.K.; Passell, L.; Taub, H.; Dash, J.G.; Novaco, A.D. (1976) Neutron scattering study of nitrogen adsorbed on basal-plane-oriented graphite. *Phys. Rev. B*, 13, 1446-1462, 01631829.

Llewellyn, P.L.; Grillet, Y.; Rouquerol, J.; Martin, C.; Coulomb, J.P. (1996) Thermodynamic and structural properties of physisorbed phases within the model mesoporous adsorbent M41S (pore diameter 2.5 nm). *Surf. Sci.*, 352–354, 468-474, ISSN 00396028.

Llewellyn, P. L.; Maurin, G. (2005) Gas adsorption microcalorimetry and modelling to characterize zeolites and related materials. *C. R. Chimie*, 8, 283–302, ISSN 16310748.

Martinez, P.; L. Giraldo, E. Vargas, J.C. Moreno. (2005) Isoperibolic calorimetric cell uit electronic integrator circuit for temperature measurement. *Instrumentation Science & Technology*, 33, 415-420, ISSN 15256030.

Menéndez, J. A. (1998) On the use of calorimetric techniques for the characterization of carbons: A brief review. *Thermochimica Acta*, 312, 79–86, ISSN 00406031 .

Moreno, J.C., Giraldo, L. (2005) Influence of thermal insulation of the surroundings on the response of the outpun electrical signal in a heat conduction calorimetric unit. *Instrumentation Science & Technology*, 33, 415-425, ISSN 15256030.

Moreno, J. C.; Giraldo, L. (2005) Setups for simultaneous measurement of isotherms and adsorption heats. *Review of Scientific Instruments*, 76, 1-8, ISSN 00346748

Moreno-Piraján, J. C.; Giraldo, L.; Garcia-Cuello, V.; Sapag, K.; Zgrablich G. (2008) Design, calibration and test of a new Tian-Calvet Heat flow Microcalorimeter for Measurement of differential heats of adsorption. *Instrumentation Science & Technology*. 36, 455-475. ISSN 15256030.

Navarrete, R; Llewellyn, P.; Rouquerol, F.; Denoyel, R.; Rouquerol, J. (2004) Calorimetry by immersion into liquid nitrogen and liquid argon: a better way to determine the internal surface area of micropores. *Journal of Colloid and Interface Science*, 277, 383–386, ISSN 00219797

O´Neil, M.; Louvrien, R.; Phillips, J. (1985) New microcalorimeter for the measurement of differential heats of adsorption of gases on high surface area solids. *Rev. Sci. instrum.*, 56, 2312-2317, ISSN 00346748

O'Neil, M.; Phillips, J. (1987) Differential microcalorimetric study of chemical adsorption processes on a microporous solid. *J. Phys. Chem.*, 91, 2867- 2874, ISSN 0022-3654.

Prauchner, M. J.; Rodriguez-Reinoso, F. (2008) Preparation of granular activated carbons for adsorption of natural gas. *Microporous and Mesoporous Materials*, 109, 581-584, ISSN 13871811.

Rios, R. B.; Silva, F. W. M.; Torres, A. E. B.; Azevedo, D. C. S. ; Cavalcante Jr., C. L. (2009) Adsorption of methane in activated carbons obtained from coconut shells using H_3PO_4 chemical activation, *Adsorption*, 15, 271-277, ISSN 0929-5607.

Rouquerol, F.; Rouquerol, J.; Sing, K. Adsorption by Powders & Porous Solids. Academic Press, San Diego, 1999.

Rouquérol, J. (1985) The contribution of microcalorimetry to the solution of problems involving a liquid/solid or a gas/solid interface, especially in physisorption. *Thermochim Acta*, 96, 377-390, ISSN 00406031

Ruthven, D. M.; Shamsuzzaman, F.; Knaebel, K.S. (1994) Pressure Swing Adsorption, VCH Publishers, New York/Weinheim,

Sharma, S.B.; Miller, J.T.; Dumesic, J.A. (1994) Microcalorimetric Study of Silica- and Zeolite-Supported Platinum Catalysts. *Journal of Catalysis.*, 148, 198-204, ISSN: 0021-9517 .

Sing, K.S.W.; Everett, D.H.; Haul, R.A.W.; Moscou, L.; Pierotti, R.A.; Rouquérol, J.; Siemieniewska, T., (1985) Reporting physisorption data for gas/solid systems with special reference to the determination of surface area and porosity. *Pure Appl. Chem.* 57, 603, ISSN 00334545.

Siperstein, F.; Gorte, R.J.; Myers, A.L. (1999) A New Calorimeter for Simultaneous Measurements of Loading and Heats of Adsorption from Gaseous Mixtures. *Langmuir*, 15, 1570-1576, ISSN 07437463.

Spiewak, B. E.; Handy, B. E.; Sharma, B.; Dumesic, J.A. (1994) Microcalorimetric studies of ammonia adsorption on γ-Al_2O_3, HNa-Y zeolite, and H-mordenite. *Catalysis Letters.*, 23, 207-213, ISSN 1011372X.

Swietoslawski, W. (1948) Microcalorimetry. Ed. Reinhold. New York.

Wadso I., (1986) Bio-calorimetry. *Trends Biotechnol.*, 4, 45-51, ISSN 01677799

Wadso, I.; Goldberg, R.N. (2001) Standards in isothermal microcalorimetry. *Pure Appl. Chem.*, 73, 1625-1639 ISSN 00334545

Wilhoit, R.C. (1967) Recent developments in calorimetry: Part two. Some associated measurements. *J. Chem Ed.*, 44, A571, ISSN 00219584.

Wirawan, S. K.; Creaser, D. (2006) CO_2 adsorption on silicalite-1 and cation exchanged ZSM-5 zeolites using a step changeresponse method. *Microporous and Mesoporous Materials*, 91, 196–205, ISSN 13871811

Yang, R. T. (1997) Gas Separation by Adsorption Processes, Butterworths, London, Imperial College Press, London, UK

Zielenkiewicz, W. (2000) Comparative measurements in isoperibol calorimetry: uses and misuses. *Thermochim. Acta*, 347, 15-20, ISSN 00406031

Zimmermann, W.; Keller, J. U. (2003) A new calorimeter for simultaneous measurement of isotherms and heats of adsorption. *Thermochimica Acta*, 403, 31 – 41, ISSN 00406031
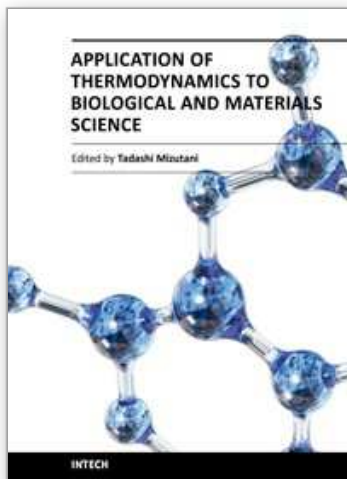
Application of Thermodynamics to Biological and Materials Science

Edited by Prof. Mizutani Tadashi

Progress of thermodynamics has been stimulated by the findings of a variety of fields of science and technology. The principles of thermodynamics are so general that the application is widespread to such fields as solid state physics, chemistry, biology, astronomical science, materials science, and chemical engineering. The contents of this book should be of help to many scientists and engineers.

How to reference

In order to correctly reference this scholarly work, feel free to copy and paste the following:

Juan Carlos Moreno and Liliana Giraldo (2011). Calorimetric: A Tecnique Useful in Characterization of Porous Solid, Application of Thermodynamics to Biological and Materials Science, Prof. Mizutani Tadashi (Ed.), ISBN: 978-953-307-980-6, InTech, Available from: http://www.intechopen.com/books/application-of-thermodynamics-to-biological-and-materials-science/calorimetric-a-tecnique-useful-in-characterization-of-porous-solid

INTECH
open science | open minds